TAMPERE UNIVERSITY OF TECHNOLOGY

Esa Kaarna

EEG analysis of Parkinson's disease patients treated with 50 Hz repetitive transcranial magnetic stimulation

Master's thesis

Tarkastaja: professori Jari Viik
Tarkastaja ja aihe hyväksytty
Tieto- ja sähkötekniikan tiedekuntaneuvoston kokouksessa 4.9.2013

TIIVISTELMÄ

TAMPEREEN TEKNILLINEN YLIOPISTO
Sähkön koulutusohjelma
Esa Kaarna: EEG analysis of Parkinson's disease patients treated with 50 Hz repetitive transcranial magnetic stimulation
Diplomityö, 51 sivua, 4 liitesivua
26.1.2015
Pääaine: Biomedical Engineering
Tarkastajat: professori Jari Viik
Avainsanat: Parkinson's Disease, EEG, AAR, EOG, EMG

Toistuva transkraniaalinen magneettistimulaatio (rTMS) on osoittanut lupaavia tuloksia Parkinsonin taudin (PT) hoidossa, mutta parhaita taajuuksia eikä parametreja sille olla vielä löydetty. Tämän työn tavoitteena oli selvittää vaikuttiko 50 Hz rTMS hoito PT potilaisiin tutkimalla ennen ja jälkeen mitattuja EEG signaaleita. Työssä tarkasteltiin myös uuden automaattisen artefaktojen poisto algoritmin (AAR) käyttöä data-analyysiin tukena. Tutkimuksen hypoteesina oli, että EEG:n beettakaistan tehospektritiheyden tulisi kasvaa hoidon myötä.

Potilaiden lukumäärä väheni lopulta kahdeksaan (n=8). Lopullinen datajoukko piti sisällään noin 20 minuuttia bipolaarista, 21 kanavaista, EEG signaalia (ennen ja jälkeen) jokaiselta potilaalta. EEG signaali mitattiin alkuperäisessä tutkimuksessa vain turvallisuussyistä, joten se piti sisällään paljon artefaktoja. Tarkasteltu AAR algoritmi oli uusi F-wICA algoritmi, joka havaitsee automaattisesti EOG tai EMG artefaktoja signaalista perustuen fraktaalidimensioihin. Artefaktojen poiston jälkeen data jaettiin tehospektritiheyksiin eri EEG kaistoille ja kanaville FFT:n avulla. Tulokset kasattiin ja tarkasteltiin tämän jälkeen Wilcoxonin testillä.

Ennen varsinaisia tuloksia AAR algoritmin käyttö arvioitiin ja todettiin sen olevan vielä kesken ja käyttökelvoton data-analyysin tukena. Tilastollisen testin tulokset käsin puhdistetulla datalla osoittivat nollahypoteesin avulla, että vain yksi tarkasteltava muutos 12 mahdollisesta (2 beetta kaistaa ja 6 EEG kanavaa) ylitti merkittävyyden rajan (< 0.05) oikeaan suuntaa. Tuloksen yksittäisyys sekä EEG datan artefaktaisuus johtivat päätelmään, että potilaiden EEG aktiivisuudessa ei havaittu merkittävää muutosta rTMS hoidon jälkeen.

Jatkotutkimuksissa EEG:n mittaamiseen tulisi kiinnittää enemmän huomiota. Sen on osoitettu havaitsevan TMS hoidon vaikutukset paremmin kuin käyttäytymistutkimukset. Tulokset ovat myös kvantitatiivisia, joten niiden vertailu on tulevaisuudessa helpompaa.

ABSTRACT

TAMPERE UNIVERSITY OF TECHNOLOGY
Master's Degree Programme in Electrical Engineering
Esa Kaarna : EEG analysis of Parkinson's disease patients treated with 50 Hz repetitive transcranial magnetic stimulation
Master of Science Thesis, 51 pages, 4 Appendix pages
26.1.2015
Major: Biomedical Engineering
Examiner: Professor Jari Viik
Keywords: Parkinson's Disease, EEG, AAR, EOG, EMG

Repetitive trancranial magnetic stimulation (rTMS) has shown promising results in treating Parkinson's disease (PD), but the best frequencies and parameters have not yet been established. The objective of this study was to determine whether 50 Hz rTMS treatment had an effect on PD patients studying the recorded EEG data before and after the treatment. A novel automatic artifact rejection (AAR) algorithm was also tested with the data analysis. The hypothesis was that the power spectral density of EEG beta band increases after the treatment.

The amount of patients eventually narrowed down to eight (N=8). The complete dataset was around 20 minutes of bipolar 21-channel EEG signal (pre and post) from each patient. EEG was recorded only for safety purposes in the clinical study, so the data was quite filled with artifacts. The AAR algorithm tried was a novel F-wICA algorithm which automatically identifies EEG containing EOG or EMG artifacts based on fractal dimensions. After the artifact rejection the data was divided into power spectral densities of different EEG bands and channels using FFT. The results were then combined and studied with Wilcoxon signed rank test.

Before the actual results, the use of AAR algorithm was assessed and it was found out not to be ready and could not be used for the actual analysis. The results of statistical analysis with only manually rejected data showed that with null hypothesis only one of 12 possible changes of interest (2 Beta Bands and 6 EEG channels) had a significant change (< 0.05) into the expected direction. That alone and the fact that the EEG data was filled with artifacts led to the conclusion that there was no notable difference of EEG activity after the rTMS treatment.

Further research should be made by focusing more on the EEG recording. It has been shown to indicate the affect of the TMS treatment better the behavioral studies. Results are also quantitative so the comparison would be easier in the future.

PREFACE

This Master of Science Thesis was made for the Department of Biomedical Engineerin in Tampere University of Technology (TUT). The thesis was made under supervision of Professor Jari Viik and MSc Atte Joutsen.

I would like to thank MSc Atte Joutsen for providing me the data for this thesis and for instructing me with the analysis. I would like to thank both of my supervisors for their help and understanding with the long prosess of me finishing with this thesis.

Tampere, 13.2.2015

Esa Kaarna

CONTENTS

LIST OF ABBREVIATIONS

TMS	Transcranial Magnetic Stimulation
rTMS	repetitive TMS
EEG	Electroencephalogram
PD	Parkinson's disease
AAR	Automatic Artifact Rejection
FFT	Fast Fourier Analysis
EOG	Electrooculogram
EMG	Electromyogram
DA	Dopamine
SNpc	Substantia Nigra pars compacta
LBs	Lewy Bodies
DBS	Deep Brain Stimulation
L-dopa	Levodopa
IPG	Implantable Pulse Generator
TES	Transcranial Electrical Stimulation
iTBS	intermittent Theta-Burst transcranial magnetic Stimulation
SNR	Signal-to-Noise Ratio
PET	Positron Emission Tomography
fMRI	functional Magnetic Resonance Imaging
PSP	Postsynaptic Potentials
ICA	Independent Component Analysis
wICA	Wavelet enhanced ICA
AIC	Artifactual Independent Comonent
FD	Fractal Dimensions
PSD	Power Spectral Density

1. INTRODUCTION

High-frequency ($>$ 1 Hz) repetitive transcranial magnetic stimulation (rTMS) has shown promising results in therapeutic use for Parkinson's disease (PD) patients. 25 Hz rTMS has been proven to improve gait which previously only responds to dopaminergic therapy [23]. rTMS stimulation is a non-invasive pain-free technique which has a great potential in being a powerful addition to conventional therapy in PD. 25 Hz rTMS has been superior to 10 Hz rTMS in previous studies [20], so it is fair to expect that even higher frequencies may excite the brain even more.

The purpose of this study was to assess the effects of the longer and higher-intensity 50 Hz rTMS of the motor cortex (M1) in PD patients using EEG data recorded before (pre) and after (post) the measurements. In addition to that, also a novel automatic artifact rejection (AAR) algorithm was tested for the cleaning of the EEG data. The EEG data came from a safety study for the 50 Hz rTMS, not considered as safe at the time, by Benninger et al. [6]. The pre- and post-EEG was recorded merely as a safety assessment in the original clinical study but as the study did not show any side-effects of the rTMS, the EEG wanted to be studied. This study is the direct successor of the safety study and the results were reported back to Benninger et al.

The hypothesis for the effect of the rTMS treatment was that the treatments should excite the brain activity on the beta band (12 Hz - 30 Hz) and hence seen as an improvement in the motor functions of the patients. Because possible subtle changes in these functions are hard to discover with behavioral studies, the EEG study should be done. The study question was then to discover whether the brain activity increase in the beta band in the population after the 50Hz rTMS treatment. The hypothesis was studied with null hypothesis (H_0) by looking for significant changes (P-value $<$ 0.05) in the results after the treatment.

The clinical study included only one treatment so the possible positive effects might be only short lived relief, however review of literature suggests that repetitive treatments might induce long term improvements [12]. For that question this study was not able to answer.

The study question concerning the AAR algorithm was to find whether it could be used in the artifact rejection process. Different AAR algorithms had been used successfully before and the AAR algorithm used in this study represented a state-of-

the-art technique on the field. The effect of the algorithm was assessed with visually studying the results and by averaging large amounts of data of the effects of the algorithm.

The first part of the thesis explains the theories behind the PD and EEG and also reviews the literature concerning TMS studies and uses of AAR with EEG studies. The pathology and the symptoms of the PD are considered but also couple of other treatment methods than the rTMS. The EEG is explained a bit more thorough and its measurements setup methods and problems with the measurements. The second part introduces the objectives and the used methods for the artifact rejections and for the whole signal processing process. The texts are supported with flow charts in the appendices section. The third section reveals the results and discusses them.

2. BACKGROUND

The background section includes the basic knowledge of the PD and EEG and presents some related studies from the field of TMS and AAR. It helps to understand results and how they relate to other research done.

2.1 Parkinson's disease

PD, also known as Paralysis agitans or Shaking palsy, is part of a group of neurological disorders called motor system disorders [36]. It most often develops after age 50 and affects both men and women, but can also occur in younger adults [1]. In Finland alone there are over 10,000 PD patients [34].

2.1.1 Pathology

PD is known to result primarily from the death of dopaminergic neurons in the Substantia Nigra pars compacta (SNpc). A loss of SNpc neurons then leads to a loss of Dopamine (DA). [36] DA is an important neurotransmitter chemical that sends signals to the part of the brain which controls movement [17]. Therefore, the absence of DA is a major cause of PD symptoms.

The pathological findings from PD patients show losses of nigrostriatal dopaminergic neurons and the presence of intraneuronal proteinacious cytoplasmic inclusions, termed Lewy Bodies (LBs) (see Figure 2.1) The cell bodies of nigrostiatal neurons are in the SNpc, and their axons project primarily to the putamen. The loss of these neurons causes depigmentation of the SNpc, which is a classic neuropathological finding suggesting PD. [36]

2.1.2 Symptoms

The most evident symptoms of PD involve difficulty in movement control due to lack of DA. The most common symptoms are tremor, stiff muscles, slow movement, and problems with balance or walking [17].

Tremor is often the first symptom of the disease, but everyone does not have it and it does not always mean PD [17]. Tremor is a sort of a muscle oscillation, which cannot be stopped. An ability to stop an initiated movement is one way DA controls our movement, so a lack of it causes all kinds of problems with PD patients,

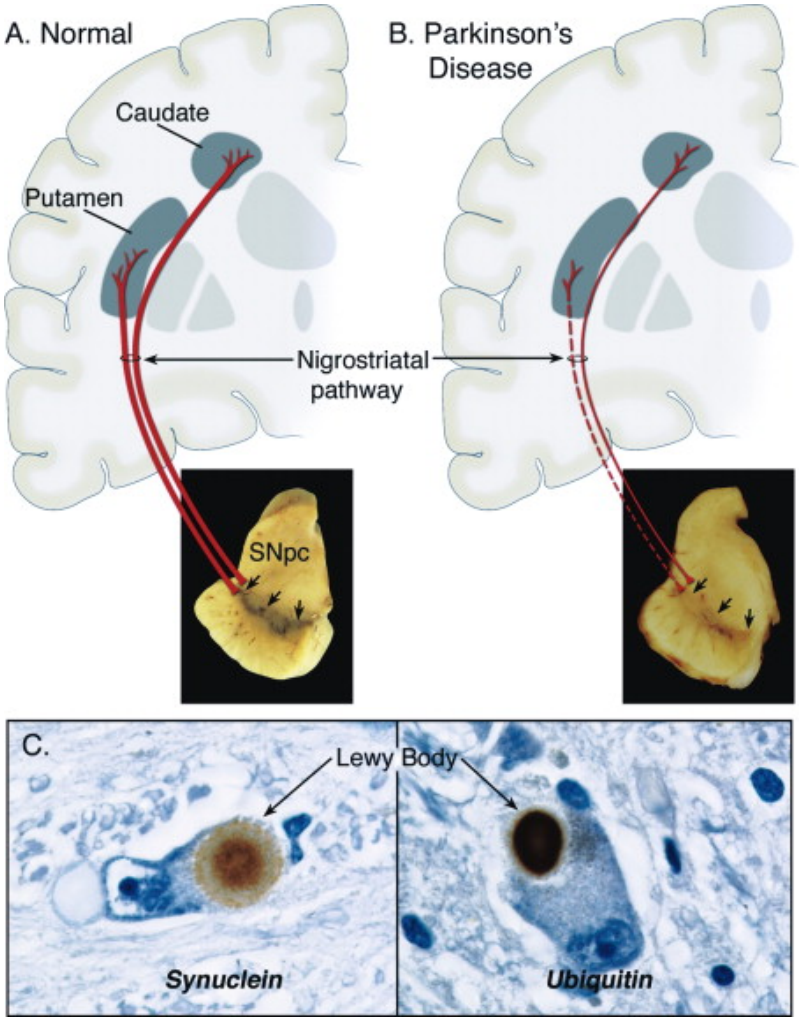

Figure 2.1: Neuropathology of PD. (A) Represents a normal nigrostriatal pathway, (B) a diseased nigrostriatal pathway and (C) shows immunohistochemical labeling of intraneuronal inclusions, in a Substantia Nigra pars compacta dopaminergic neuron. [36]

for example slow movement and falling.

Eventually PD progresses so that it affects the facial muscles and the patients have problems with swallowing or showing facial expressions. This causes difficulty in communication and may look like mental degeneration. Some people actually do have a decrease in mental skills, like dementia, due to PD [17].

2.1.3 Treatment methods

PD is thought to be caused by a lack of DA, so the primary therapy involves DA replacement drugs. Drugs do ease the symptoms, but the degeneration of non-dopaminergic neurons progresses and cause symptoms which are not affected by a conventional therapy. Some symptoms may be disabling in advanced PD, like difficulties with gait and periodic falls. Researchers are trying to discover invasive and

noninvasive treatment methods, like invasive Deep Brain Stimulation (DBS) and noninvasive rTMS, and the results are promising. Controlled rTMS studies have already demonstrated gait improvement, which has led the researchers to consider more powerful stimulation protocols. [4]

Drugs

Because the main reason for PD is the lack of DA, the aim of the medication is to deliver DA to the brain. Usually patients are treated with Levodopa (L-dopa), which is a precursor for DA. It has an ability to cross the blood-brain barrier, but DA itself has not. L-dopa is often combined with carbidopa, which delays the conversion from L-dopa to DA. [13]

L-dopa treatment is the most effective treatment for the motor symptoms, but it does not apply to all patients nor all the symptoms. Especially problems with balance and tremor are often not improved as expected, but bradykinesia (slow movement) and muscle rigidity are. [13]

There are also other drugs in trial such as Bromocriptine, Pramipexole and Ropinirole, which are similar to DA and the neurons react to them in the same way. However, these are still under investigation. [11]

Deep Brain Stimulation

DBS is an invasive surgical treatment method, where an electrode is introduced deep into the brain. The same method is also used for depression and some other mental disorders.

The device consists of an electrode, wire, and an electrical control unit named Implantable Pulse Generator (IPG). The electrode is surgically placed in the brain with a wire connected outside the body and to the IPG. The control unit is then attached under the patients' skin, usually near the collar bone. The IPG sends high frequency pulses to the electrode and therefore stimulates the brain. [43]

The brain is so complex that it is impossible to know for certain where to put the electrode, but the researchers have used a basic trial and error method to find some useful target areas in subthalamic nucleus which have an effect on PD [43]. Also the optimal electrical stimulation procedure needs to be found by trial for each patient.

Despite the obscure nature of the treatment, it has proved some major effects on the PD and the method is in trial use. Especially symptoms like tremor, slowness of movement, and stiffness of muscles can be treated with the DBS. It can also reduce the amount of the L-dopa needed and minimize its side effects. [11]

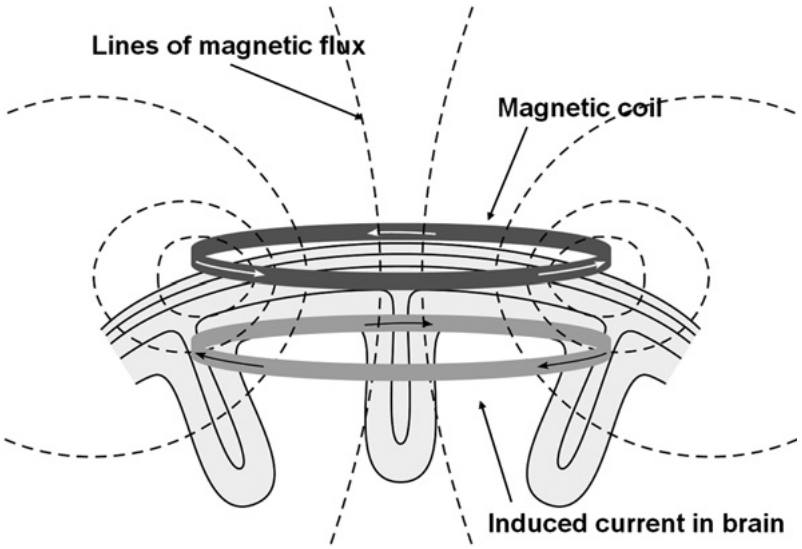

Figure 2.2: Illustration of direction of current flows in a magnetic coil and the induced current in the brain [16].

Transcranial Magnetic Stimulation

TMS is quite a recent and powerful tool for studying the human brain. A magnetic field induces a current flow in the brain that can excite or inhibit wanted areas. This procedure is illustrated in Figure 2.2. TMS can be used as a stimulus exhibitor, inhibitor, or it can alter the functions of the brain beyond the time of stimulation, thus offering potential for therapy. [15]

The technique was discovered around three decades ago. It was started as a brief, high voltage electric shock that activated the motor cortex (a part of the brain that controls the movement) uninvasively. It was called Transcranial Electrical Stimulation (TES). [30] The only drawback was that it hurt, because the shock also activated some pain receptors. Then five years later researchers discovered a way to stimulate the brain using an external magnetic stimulation with a little or no pain. It was then called Transcranial Magnetic Stimulation. [2] TMS is now a widely used research tool and also a potential tool for therapeutic purposes. [15]

There are two main variables with the TMS, stimulation signal and the magnetic coil used. The coil affects the stimulation area and the stimulation signal the stimulus itself. The type of coil is not important in this context, but it is good to know that the coil for PD treatment is often a single round coil. The more important variable is the stimulation signal.

Researchers are still experimenting with different kinds of stimulation methods for PD treatment purposes. So far the repetitive TMS (rTMS) [6] and the intermittent Theta-Burst transcranial magnetic Stimulation (iTBS) [4] have showed promising results. Now the researchers are further experimenting with repetition frequencies

and pulse lengths, so there is still plenty of research ground to cover.

Granted that TMS treatment is a relatively new method, it has shown promising results in improving gait with PD patients [23]. Researchers are hoping to create a therapeutic tool with TMS, so that the patients would only need to come to the hospital and receive the treatment without any discomfort or pain. Then leave with a little improvement in coping with daily tasks. Researchers like Benniger et al. [6] have already proven the rTMS treatment to be safe with different frequencies all the way up to 50 Hz.

2.2 Electroencephalography

The human brain is the most complex and advanced organic mass ever researched by a man. For this reason, and the fact that our brain makes us *us*, the research around the brain has been really intense and extensive. [38, p. 25] Particularly problematic for the research have been the sensitivity and the measurability of the brain. It is hard and dangerous to set measuring equipment into a living brain tissue and on the other hand a dead brain tissue does not have any measurable cognitive abilities.

One way to avoid this problem is to measure the brain using a non-invasive measuring equipment, like electroencephalography (EEG), which measures the electrical activity of the brain from the scalp using a set of electrodes [32, pp. 139-143]. Even this is not quite straight forward because the further the electrodes are from the brain the weaker the signal gets; furthermore, the weaker the signal gets the worse the signal-to-noise ratio (SNR) gets.

2.2.1 History

In the year 1875 Richard Caton discovered that weak (microvolt range) electrical signals can be measured on the cerebral cortex of rabbits and dogs [38, p. 25]. Several years later, a German researcher Hans Berger recorded electrical "brain waves" for the first time by attaching electrodes to the human scalp. He discovered that the waves had a time-varying, oscillating behavior that differed depending on the measurement location on the scalp. He also found out that the brain waves differed between healthy and neurologically diseased patients and between different mental states, like attention, relaxation, or sleep. These experiments led Berger to discover the alpha waves and to named his equipment as *electroencephalogram* [7].

Berger's realizations and experiments laid the foundation for EEG, which is still today an important noninvasive clinical tool to measure and understand the structure and the functions of the brain. EEG itself is not self-explanatory but it needs a human reader who draws conclusions from it based on the frequency, amplitude, morphology, and spatial distribution of the brain waves. EEG interpretation re-

mains a phenomenological clinical discipline because no biological or mathematical model has been able to fully explain its patterns. Modern and powerful computers have brought a new dimension to the EEG measurements in the form of signal processing. The data handling can be almost completely automated but the final interpretation still depends on the human view. [38, pp. 25-26]

Modern technology allows more effective ways to measure the brain than EEG, like Positron Emission Tomography (PET) and functional Magnetic Resonance Imaging (fMRI), but it still remains a very powerful tool in the diagnosis of many diseases. Although, EEG is relatively hard to read, the researchers have vast experience and data from the past decades. [38, p. 26] Furthermore, EEG has a great time resolution, which is important for real-time monitoring, but unfortunately a bad volume resolution. With imaging methods, like fMRI and PET, the characteristics are just the opposite. For this reason, best results can be obtained with combining EEG with an imaging method. Another advantage with EEG comparing with imaging methods is that it measures the activity of the neurons directly, where imaging methods measure the event indirectly studying the metabolism of the nervous tissue. [35, pp. 50-64]

2.2.2 Characteristics

The signal obtained from the EEG measurements is really obscure and researchers are not even in this day certain where or how deep from the brain it comes from. According to Partanen [35, p. 50], the brain activity seen in the EEG arises mainly in the cerebral cortex but there is a constant debate on the actual measurement depth of the EEG. It is known that the cerebral cortex has a thickness of 2-3 mm and wavy neuronal area of 2.5m^2, so it includes more than 10 billion signaling neurons [38, p. 30]. The signals of individual neurons are so weak, that they need to act as a large synchronized group to be detected with the EEG. On the contrary the asymmetry of the neuronal signals attenuates the detectable signal because the opposite charges cancel each other out.[32, p. 109]

The action potentials propagating in the axons cannot be seen with the EEG, because they are too fast (around 1 ms) to happen in synchrony. Additionally a propagating action potential forms an electrical quadrupole, two near and opposite dipoles, which electric and magnetic fields attenuate as a function of distance [35, p. 50]. The EEG waves mainly picture the electric fields generated by currents that flow during synaptic excitation of the dendrites, the synchronic Postsynaptic Potentials (PSP), which usually last for several milliseconds [38, p. 31]. The PSPs often form only parallel dipoles, whose electric and magnetic fields attenuate one order of magnitude slower as a function of distance than quadrupoles [35, p. 50].

The intensity of the electrical field in the EEG does not necessarily correlate to

the intensity of the neuronal communication because it only records the parallel events. In fact, when the neuronal activity is at its highest, the intensity of the electric fields is at its lowest because the neurons are performing different tasks in a smaller groups [38, p. 32]. Similarly as the neurons act in synchrony, the electric field is great and oscillating, and the neuronal communication is relatively minor. In fact, in this kind of state one is in a dream like state or relaxed. For this reason, the oscillating EEG data is used to diagnose different sleep states and detecting coma [25].

2.2.3 Measurement setup

The International EEG congress decided in 1949 to standardize the measurement of EEG because the placement of electrodes and naming differed slightly between the various institutions [21]. A common standard allowed the comparison of the results, and ensured the accuracy of the measurements.

The placement standard of the electrodes was named as 10-20 system. The system is based on the relative locations of electrodes from one another. The distance between the low forehead and the back of the head (from nasion to inion) and between the left ear and the right ear are measured and the electrodes are located into 10% and 20% intervals along these measurements. [35, p. 71] This way the size of the head does not affect the measurements dramatically. The locations of the electrodes are furthermore named after the parts of the brains they are over, to help the identification of the measurement points. Figure 2.3 clarifies the placement and the naming of the electrodes. Today the 10-10 system is already used, where the electrodes are located tighter, but the 10-20 system is still in parallel use in the clinical routine.

The electrodes of the EEG can be used to measure either by unipolar or bipolar. In the unipolar measurements, the signal is recorded from one electrode to the reference electrode, which is either positioned distantly or taken as the average of all electrodes. This measures the activity of the brain around one measurement point. In the bipolar measurements, the signal is recorded from one electrode to another. This measures the activity of the brain in the region between the two electrodes. [38, p. 37]

The electrodes used in the EEG are located on the scalp but they measure the electrical activity of the brain. This means that the signal needs to travel through a heterogeneous mass before it is measured [25]. The mass of the brain alone attenuates the signals that are born deeper inside the brain but the signals also need to travel through the cerebrospinal fluid, bony skull, skin, and hair. The electrical conductivity of the skull is approximately two orders of magnitude weaker than that of brain tissue, so it acts as a strong absorber [35, p. 51].

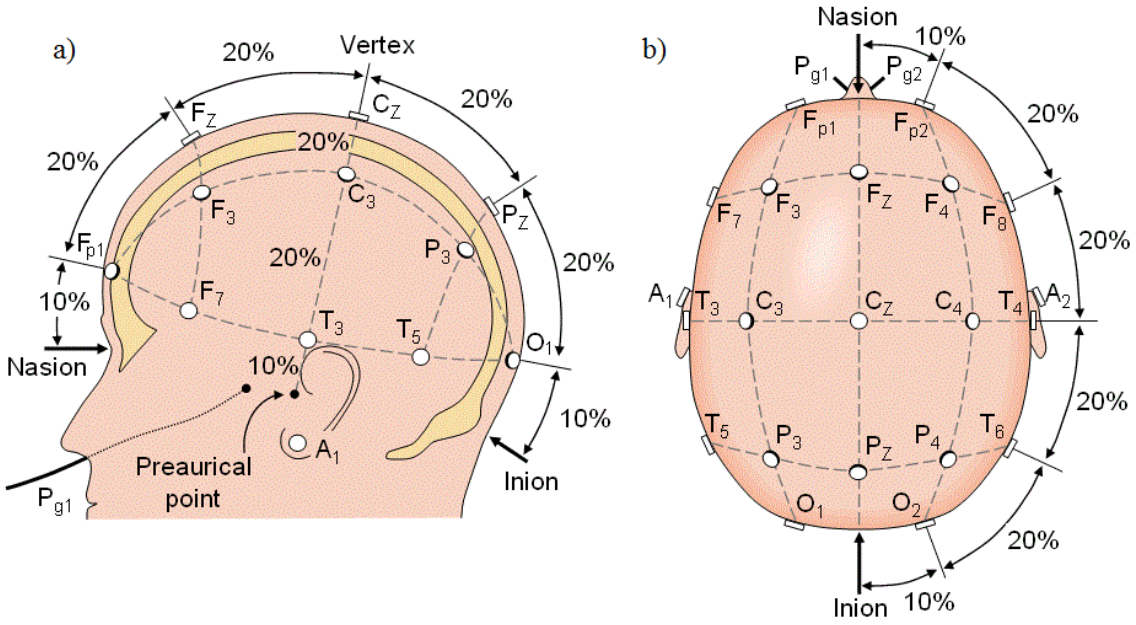

Figure 2.3: International 10-20 system seen from a) left and b) above the head. A = Ear lobe, C = central, Pg = nasopharyngeal, P = parietal, F = frontal, Fp = frontal polar, O = occipital, T = temporal [25].

2.2.4 Artifacts

The measurement results are affected in addition to attenuations by various external interference and other body signals. These artifacts bring information to the measurements, which are not origin from the brain. For this reason they need to be avoided completely or removed from the final data with rejection or filtering.

Ambient artifacts are for example 50/60Hz network noise, electrode artifact, signal filtering artifact, equipment artifact, and electric and magnetic field artifact. The electrode artifact can be seen in the data as a short term amplitude fluctuations due to impedance changes of the poorly attached electrodes. The signal filtering and equipment artifacts, however, may distort the EEG due to wrong sampling frequency or unnecessary filtering. The electric and magnetic field artifact affect the EEG in a wide frequency spectrum, because they connect to the patient through many electric sources that are located in the same room where the measurement is done. [35, pp. 104-106] They can induce current into the measurement cables either by magnetic fields or due to the movement of the patient. Ambient artifacts can be avoided with a proper planning and the selection of the location.

The patient related artifacts are especially problematic because they cannot be affected by planning. It is almost impossible for a healthy person to be absolutely still during the measurements purely because of involuntary movements. Even more problematic is to measure the cognitively ill patients, which the researchers are often

more interested in, because they have even more involuntary movements, spasms, or tremors.

Especially challenging artifacts for the EEG measurements are the head area artifacts. The patient may unintentionally bite his jaws together or move his eyes. Every muscular movement causes Electromyographic (EMG) signal, which is more powerful than EEG and adds on top of it covering the EEG partially or completely. In addition to EMG, eye movement causes Electrooculogram (EOG), which is seen in the EEG data as huge amplitude changes and peaks. The EOG is caused by the potential difference between the cornea and the retina which changes during eye movement [38, p. 74].

Another eye based artifact is the blink artifact. It is caused by the moving eyelid, which is seen in the data as huge and short amplitude peaks. They are relatively easy to detect and remove from the EEG data because they are really rapid and strong. [35, pp. 98-102]

2.3 Review of literature

Review of literature was done using Pubmed and Google Scholar to find related articles from the field. Review of literature was divided in to sections: TMS studies and AAR algorithms with EEG.

2.3.1 TMS studies

First reviewed article was a systematic review article made by Guse et al. [14]. They performed a systematic literature search using PubMed and MEDLINE and eventually reviewed 30 out of 80 hits. Their goal was to get a good view on the cognitive effects of high-frequency TMS so they focused on the cognitive results rather than EEG or EMG results.

They immediately found a consistent problem from the field that cognitive assessments in the studies differ [14]. There is no standardized cognitive test battery jet in the field so different results are hard to compare. This is a problem in which will in the future hopefully be a solution.

Guse et al. divided their finding in two groups: low-frequency ($<$ 1 Hz) and high-frequency ($>$ 1 Hz) rTMS. They found out that low-frequency rTMS is likely to cause inhibition of neuronal firing in a localized area, whereas high-frequency rTMS does the opposite, excites the neurons by depolarization [14]. This is a finding which seems to be consistent throughout the field as also demonstrated by Thut et al. [41] in their review article reviewed next and Schindler et al. in their study of theta burst TMS associated with increased EEG synchronization [37]. This seems to be due to the low-frequencies tendency to excite large areas of neurons to act as

a unison which according to Schindler et al. may interfere with cortical information processing and be correlated to an impaired behavioral performance of the brain [37].

The conclusion of Guse et al. was that many of the studies failed to demonstrate significant cognitive effects with any frequency of rTMS, but they could show trends toward selective cognitive improvements [14]. Concerning the cognitive outcome they found out that high-frequency studies seem to be superior in comparison to the low-frequency studies [14]. At the moment of their literature review only frequencies up to 20Hz had been used because higher frequencies were not considered safe at the time so it was jet to be discovered how even higher frequencies compare. Another missing angle of research in the papers they reviewed was the length of the effect period on the patients. At the time of their article it was believed that the effects of the rTMS treatment did not last long but were merely a short term aid.

Another reviewed article was again review article about TMS-EEG studies to characterize lasting effects of rTMS and assessing their usefulness in cognitive and clinical neuroscience by Thut et al. [41]. They used PubMed and references from relevant articles to find out more than 100 studies from which they studied 51 experiments [41]. The main difference to the previous article was that Thut et al. believed EEG activity to be more sensitive measure for evaluating TMS-impact on brain function than behavioral effects so they collected the results of EEG changes rather than behavioral effects [41].

The results of Thut et al. suggest that TMS does affect a specific component of the EEG potentials depending on site of stimulation and that higher TMS-frequencies ($>$ 5 Hz) seem to be more effective than lower frequencies ($\sim$ 1 Hz) [41]. Thut et al. also considered the duration of the effects of the treatments and found out that no study suggests effect duration over 70 minutes [41]. However, they pointed out a study by Maeda et al. [24] where they found out that the effect of rTMS session on corticospinal excitability was grater when applied 24 h after an initial session. Although there were no longer EEG or behavioral signs of the initial treatment there appeared to be a neurophysiologic trace of the first rTMS session which conditioned the impact of the second session [24]. Thut et al. also referred to a review article by Fregni and Pascual-Leone [12] who researched lasting effects of the rTMS and another noninvasive brain stimulation technique and found out that daily sessions of rTMS applied for 5 and up to 20 days could have profound relevance for therapeutic use for example for PD patients [12].

Exactly that was the goal of Benninger et al. when they tried to find whether intermitted theta-burst TMS (iTBS) [4], another TMS protocol, or very high-frequency (50 Hz) rTMS [5] were effective in the treatment of motor symptoms in PD with repetitive sessions. The data for this thesis was obtained from the precursor of those

studies, a safety study of 50 Hz rTMS in patients with PD by Benninger et al. [6]. Although Benninger et al. did not find any neurophysiological or neuropsychological changes in their PD patients after rTMS (or iTBS) sessions they also wanted to know whether there was any change in the EEG recorded after the treatment in comparison to the recordings before. The thought of Thut et al. introduced before support this hypothesis in stating that EEG activity might be more sensitive measure for the effects of rTMS than cognitive or physiological tests [41].

2.3.2 Automatic Artifact Rejection algorithms with EEG

EEG signals are almost always contaminated with different artifacts such as signals of ocular and muscular origins. Such artifacts are especially present with patients who suffer from cortical disorders such as PD or Alzheimer's disease (AD). Artifact removal techniques often rely on the expertise of the EEG technician to visually detect and remove these unwanted components of the EEG signal. With large datasets the task becomes extremely laborious so automated procedures have been developed to ease the task. They should be faster, easy to use, and more objective.

In their paper in 2009 Tran et al. compared an automated artifact removal method with the then current standard method of subjectively choosing artifact components using visual detection [42]. Their AAR was performed using data obtained from a 32 channel EEG recording of 40 seconds duration [42]. They used EEGLAB [9] to apply filters on the data to remove linear trend and line noise with its harmonics and to generate ICA components using the Second Order Blind Identification (SOBI) method [3].[42] Then the data was sent to both an EEG technician who removed the artifacts using subjective visual technique and their AAR algorithm after which the comparison between the two methods was made [42].The results of Tran et al. showed that components chosen by both techniques overlapped well meaning there was no significant difference [42].

Whereas Tran et al. used real EEG data Mammone et al. [26] used an artifact-free eight-channel EEG data obtained from an online database. They wanted to present a then novel technique called Automatic Wavelet Independent Component Analysis (AWICA) and compare it to a "wavelet enhanced" ICA method [26]. Tran et al. added the artifacts to the EEG data artificially so that they would then exactly know where to look for the positive changes and how the EEG signal should look like after the artifact removal [26]. They used four different kinds of artifacts: electrical shift, linear trend, temporal muscle, and eye blink [26]. This is a great technique in assessing the effects of the AAR because the artifacts are easier to control. AWICA did show very good artifact suppression in their research and outperformed the then recent techniques which gives hope to the fully automated wavelet ICA being effective and useful in the future [26].

In a quite resent study Cassani et al. (2014) [8] investigated the effect of three state-of-the-art AAR algorithms on AD diagnostic systems. Like said before, AD is a cortical disorder like PD so they compare quite well. The three AAR algorithms were statistical artifact rejection (SAR), blind source separation based on second order blind identification and canonical correlation analysis (BSS-SOBI-CCA), and wavelet enhanced ICA (wICA) [8]. Their data included 20-channel resting-awake EEG data from 59 participants [8]. Cassani et al. also pointed out that in their studies with the same dataset two popular algorithms, the ADJUST (Automatic EEG artifact Detection based on the Joint Use of Spatial and Temporal features) [31] and FASTER (Fully Automated Statistical Thresholding for EEG artifact Rejection) [33], seemed to lead to over rejection of components, thus negatively impacting diagnostic performance [8].

The results of Cassani et al. showed that wICA outperformed all the other algorithms [8]. They also showed that the algorithms outperformed in the disease progression monitoring task in comparison to a diagnostic system trained on artifact-free data processed by human experts [8]. These resent findings give hope to the research in finding well-performing AAR algorithms to help the clinicians to go through vast amounts of data.

3. RESEARCH MATERIALS AND METHODS

The EEG data from the clinical study made by Benninger et al. [6] was not originally meant to be further analyzed but to act as a safety assessment tool. For that reason the signals were quite filled with artifacts and lacked cohesion and a lot of work was done for the data just to get it free from artifacts and coherent enough for the analysis.

The three cases of different datasets for the assessment of the therapeutic effect of the rTMS treatment used in this context were: raw data, manual rejection and manual rejection combined with AAR. The datasets are explained in this section and the results presented in the next. The flow charts of data processing stages for every case are available in the Appendices section.

3.1 The clinical study

Objectives of the clinical study made by Benninger et al in National Institute of Health (NIH) in USA at 2008 was to find a safety limit of 50 Hz rTMS [6]. rTMS had shown promising results in treating PD, but the best values for rTMS parameters had not been found. Before the study only frequencies less than 25 Hz had been investigated and the hypothesis was that higher frequencies might work better against PD, but the higher values exceeded the then current safety limits. So before the actual study the researchers needed to make a safety study for the higher frequency to evaluate its effects on the patients.

The stimulation was applied using a circular coil on the primary motor cortex (M1). Stimulation intensity was first tested at 60% rest motor threshold (RMT) and 0.5 s train duration and then increased in 0.5 s steps to 2 s, and by 10% steps to 90% RMT. During the measurements a multi-channel EMG was recorded to control for signs of increasing time-locked EMG activity, which might be an indication of an epileptic seizure, and the spread of excitation. Pre and post assessments were done with EEG, Unified Parkinson Disease Rating Scale (UPDRS), Grooved Pegboard Test, Serial Reaction Time Task (SRTT), Folstein Mini-Mental Status Examination (MMSE) and Verbal Fluency to control for motor and cognitive side effects. [6] One should note that the EEG was not used for post analysis, but merely for safety assessment.

Conclusion of the study was that 50 Hz rTMS at an intensity of 90% RMT for

a 2 second period appeared safe. Although, further research needs to be made with caution and proper EEG screening. [6]

3.1.1 Further research

The objective of this thesis is to study the pre- and post-EEG measurements to find indications that the rTMS had an effect on the patient. According to the findings of Guse et al. [14] and Schindler et al. [37] presented in the literature review, the expected outcome would be that the spectral density of the EEG should be higher in the beta-band (12Hz - 30Hz) after the high frequency rTMS stimulation. The effect of the treatment is valuated with statistical null hypothesis (H_0). If the spectral densities between pre and post measurements differ significantly ($P < 5\%$), we can state that the treatment did have an effect. The EEG is divided into EEG bands from delta to gamma band with the beta band split in two (low beta (12Hz - 20Hz) and high beta (20Hz - 30Hz)) to evaluate the effect more accurately in that band.

We were also asked to study the EEG around the stimulation frequency (50 Hz), because Benninger et al. wanted to see if the stimulation had a direct effect on that band. For this reason we separated that band (49 to 51 Hz) from the gamma band. The band was restricted to such a narrow band due to a signal loss caused by the 60 Hz notch filter, which effect was carefully evaluated using filter characteristics and signal analysis in section 5.2. The effect of the filter can be seen in the figure 3.8.

3.1.2 EEG Channels

The bipolar EEG channels of interest are F4-C4, C4-P4, F3-C3, C3-P3, Fz-Cz, and Cz-Pz with channel labels 10, 11, 14, 15, 20, and 21, respectively [6]. The channels were measured bipolarly in the initial study for an unknown reason, but it did not affect the analysis. The formation of the channels can be seen in Figure 3.1.

Although, the stimulation was applied only on the left motor cortex (M1), which includes channels F3-C3 and C3-P3, we were also asked to study the channels on the other side of the head. This way we can assess whether there is a difference between the stimulated and unstimulated side or if the effect is also mirrored to the other side of the brain. In their paper, presented in the literature review, Schindler et al. came to a conclusion that: "One might hypothesize that TBS not only has local but also remote effects and that these remote affects are probably mediated via interhemispheric inhibition. [37]" So their findings support this hypothesis.

3.2 Subject data

The patients were 5 women and 5 men, mean age 62.6 $\pm$ 9.6 years, range 50$-$77 years, 9 right$-$handed and 1 ambidextrous. They had mild to moderate PD (Hoehn

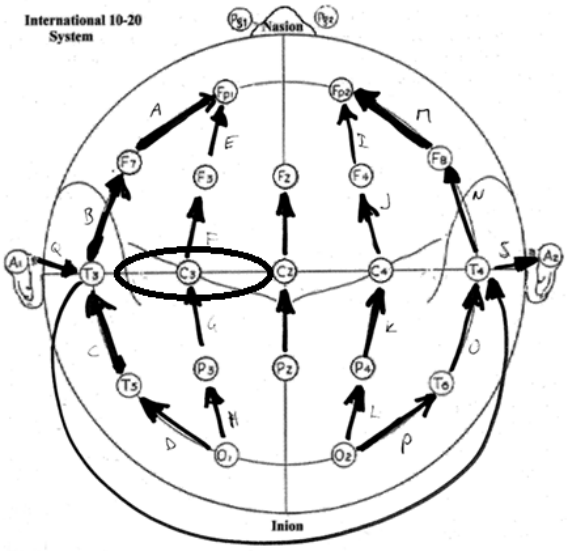

Figure 3.1: Formation of bipolar EEG channels. Black lines indicate the connected channels and their polarity. The black ellipse indicates roughly the stimulated area (left motor cortex M1). [10]

and Yahr stage mean 2.3 ± 0.4 in "on" and 2.7 ± 0.3 in "off" medication state). [6]

The EEG was recorded just for safety purposes, which meant that it was not measured with as much care as if the EEG would have been recorded for post analysis. Measurements were done at least a day before stimulus (Pre) and within 10−30 min after the last 50 Hz rTMS train (Post) and reviewed by an experienced electroencephalographer to exclude epileptic discharges or other pathological EEG phenomena [6]. The data consisted of pre and post stimulus measurements from ten patients.

The measurements were done with two different equipments (XLtek and Nihon Kohde), so the data from the two equipments needed to be analyzed separately. In addition one patient was recorded with both equipments, so the pre and post data were not comparable and the data from that patient could not be analyzed. It limited the amount of patients into nine (9).

One more patient needed to be excluded because of corrupted data. At first glance the data from different channels looked strangely coherent and noisy and not like EEG should. Finally spectral analysis confirmed that the data did not have EEG characteristics. The graph should look like a nice descending curve, but as can be seen from figure 3.2 the data does not have any EEG characteristics what so ever.

Another noticeable abnormality is that one channel has a significantly weaker signal power than others. This was also seen with other patients, but it did not affect the analysis because the channel was not of interest. It was merely another

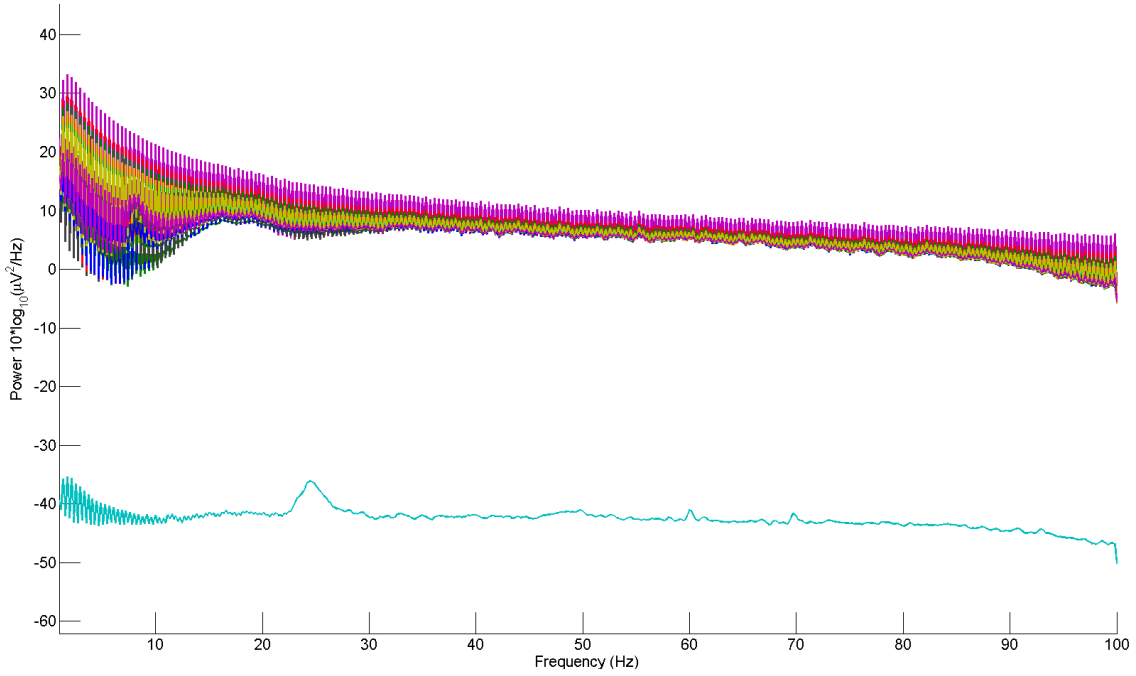

Figure 3.2: Frequency spectrum of all the EEG channels of the corrupted patient plotted in the same figure. One channel had also weaker signal and is for that reason significantly lower than others.

remainder that the data had some issues which needed to be found and dealt with.

All data files and their characteristics are collected into table 3.1. Most important columns in the table are ”Form”, which differentiates the equipment used, ”SHORT” and ”AMPSAT”, which tell the amount of corrupted data points (SHORT meaning short circuit and AMPSAT meaning amplitude saturation of the signal), missing channels, which there were some, and the type of artifact there were in the measurements. Also note that not all of the mentioned artifacts were removed during the manual preprocessing.

3.3 Manual preprocessing

The preprocessing of the data turned out to be really crucial for the EEG analysis of the data. One approach would have been to just leave the data as it was and do the frequency analysis for the ”raw” data. This would mean that some significant artifacts in either pre or post measurements might change the results. In some sense the data would be more ”genuine” and the results would consist not only EEG but also some behavioral symptoms of the patient, which could be part of the disease and so forth the results.

That approach is really hard to validate so it was decided to clean the data as good as possible using manual and automatic methods. There were such a great

Table 3.1: Charachteristics of the data files collected into one table.

File	Form	Date	Time	Post-Pre	SHORT	AMPSAT	Cha	Missing	Type of artifacts
2506 baseline 043008	txt	30.4.2008	9:24:33	4:14:25	20306	13540	32	-	Gigantic fluctuations
2506 post-50hz 043008	txt	30.4.2008	13:38:58		0	40426	32	-	Gigantic fluctuations and distortions
5570 baseline 052708	txt	27.5.2008	10:44:10	3:53:03	10304	344	32	-	A lot of EMG
5570 post-50hz 052708	txt	27.5.2008	14:37:13		10304	16812	32	-	A lot of EMG
5582 baseline 050708	txt	7.5.2008	11:13:59	3:54:28	0	925	32	-	Relatively good data, lots of blinks
5582 post-50hz 050708	txt	7.5.2008	15:08:27		0	246	32	-	Relatively good data, long, lots of blinks and some EMG
5891 baseline 031208	m00	12.3.2008	9:57:02	4:27:24	-	-	21	T3-A1	Really good, some EMG bursts
5891 post-50hz 031208	m00	12.3.2008	14:24:26		-	-	20	T3-A1	Excellent, some EMG bursts
5952 baseline 050708	txt	7.5.2008	13:52:41	23:45:07	0	2071	32	-	Horrible, lots of everything
5952 post-50hz 050808	txt	8.5.2008	13:37:48		0	0	32	-	A lot of small frequencies and EMG
6045 baseline 051308	txt	13.5.2008	14:57:25	23:28:48	0	901	32	-	Guite bad, lots of small frequencies
6045 post-50hz 051408	m00	14.5.2008	14:26:13		-	-	21	T3-A1	Excellent, some clear EMG bursts
6344 baseline 042308	m00	23.4.2008	15:00:07	22:44:46	-	-	22	-	Quite good, lots of small gaps and one huge
6344 post-50hz 042408	m00	24.4.2008	13:44:53		-	-	22	-	Quite good, lots of EMG
6373 baseline 063008	m00	30.6.2008	10:29:43	3:47:25	-	-	20	T3-A1	Excellent, some blinks, few EMG
6373 post-50hz 063008	m00	30.6.2008	14:17:08		-	-	20	T3-A1	Good, few gaps, Pz Channel goes wild
6410 baseline 060408	txt	4.6.2008	9:47:05	3:53:00	10304	7110	32	-	Quite bad, a lot of blinks and distortion
6410 post-50hz 060408	txt	4.6.2008	13:40:05		0	0	32	-	Too consistent, may be invalid
6423 baseline 070908	m00	9.7.2008	9:24:05	3:59:11	-	-	20	T3-A1	Really good, some EMG bursts
6423 post-50hz 070908	m00	9.7.2008	13:23:16		-	-	20	T3-A1	Good, but lots of blinks

artifacts and distortions in the data that some manual preprocessing was necessary. The EEG was buried so deep behind the artifacts that it was not salvageable and because there was minutes of data from each patient, there would still be minutes of data to analyze.

Manual processing was started with removing the headings of the files using a free and fast text file processing software called EditPad Lite (Just Great Software Co. Ltd.). Removing the headings helped to import the files into Matlab, because Matlab could not distinguish the headings from the data rows. Another problem with the data files was that the signals were in some cases and timeframes with the other equipment saturated or shorted. Saturation was marked in the data as strings "AMPSAT" and shorting as "SHORT". That also meant that Matlab could not import the files as they were, because there were string-variables in the middle of the data. The amount of these strings in the files can be found in table 3.1.

EditPad Lite was also good software to remove the strings with, because it works really fast for huge text files. Strings "AMPSAT" were simply replaced with values 16 and stings "SHORT" as -16. That made it possible to import the files into Matlab but also to spot them manually from the data, because no other data values were above those values and this way they formed "flat EEG segments" in the data seen in Figure 3.3.

After the data was importable into Matlab the actual manual rejection was done with EEGLAB. EEGLAB is an interactive open source Matlab toolbox for processing continuous and event-related EEG, MEG and other electrophysiological data, created by Arnaud Delorme and Scott Makeig from the University of California San Diego, Institute for Neural Computation [9]. It is also used in this work to compute Independent Component Analysis (ICA) in the AAR section.

The data was imported into EEGLAB and all the channels plotted simultaneously in the graphic interface. The interface allows the user to reject segments of the EEG including all the channels, which was great for the manual rejection. Every recording was gone through and really bad segments removed. Some cases can be seen and explained in the following figures from 3.3 to 3.7. The rejected segments are highlighted in the figures. Finally, the amount of manual rejections in samples and percentually can be seen in the table 3.2.

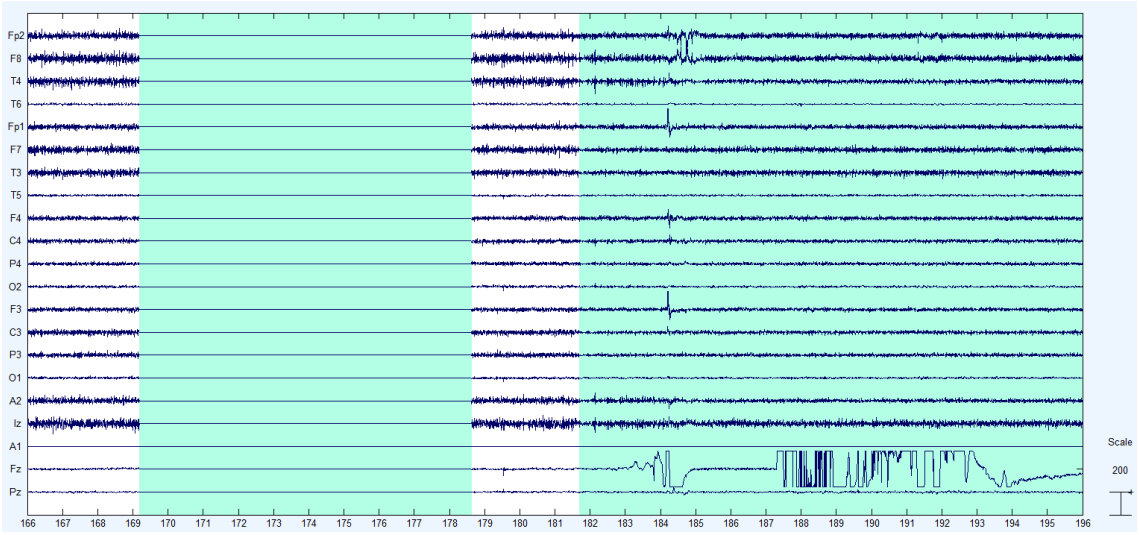

Figure 3.3: On the left a saturated "flat EEG segment", which was originally marked in the data as "AMPSAT',' and some distorted EEG on the right in channel Fz-Cz.

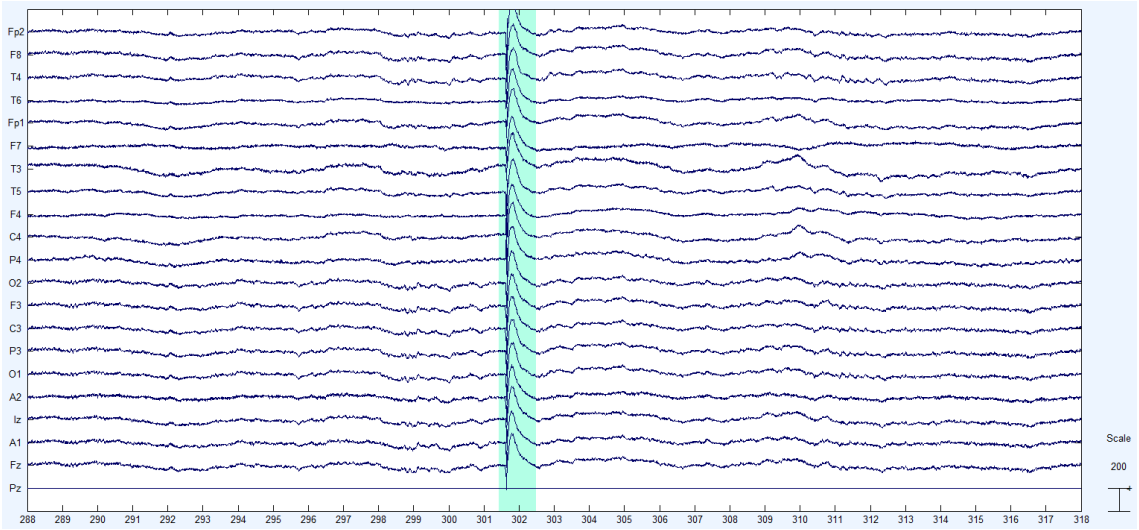

Figure 3.4: A technical artifact seen throughout the channels, which corrupts the EEG in that time frame.

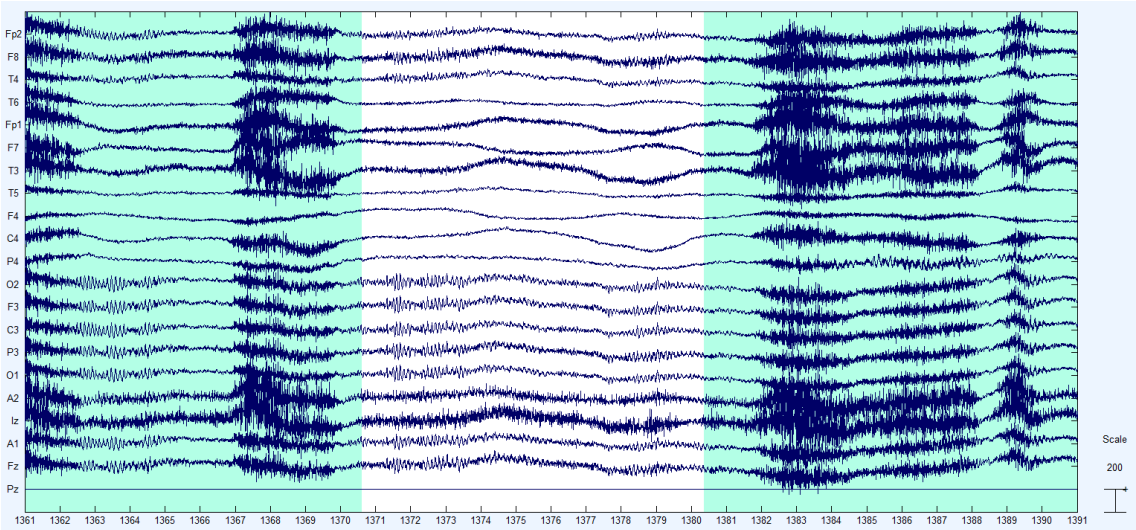

Figure 3.5: Heavy EMG contamination on both sides of the figure, which overwhelm the EEG too significantly. Middle section was quite consistent with the other parts of the current data so it was left intact.

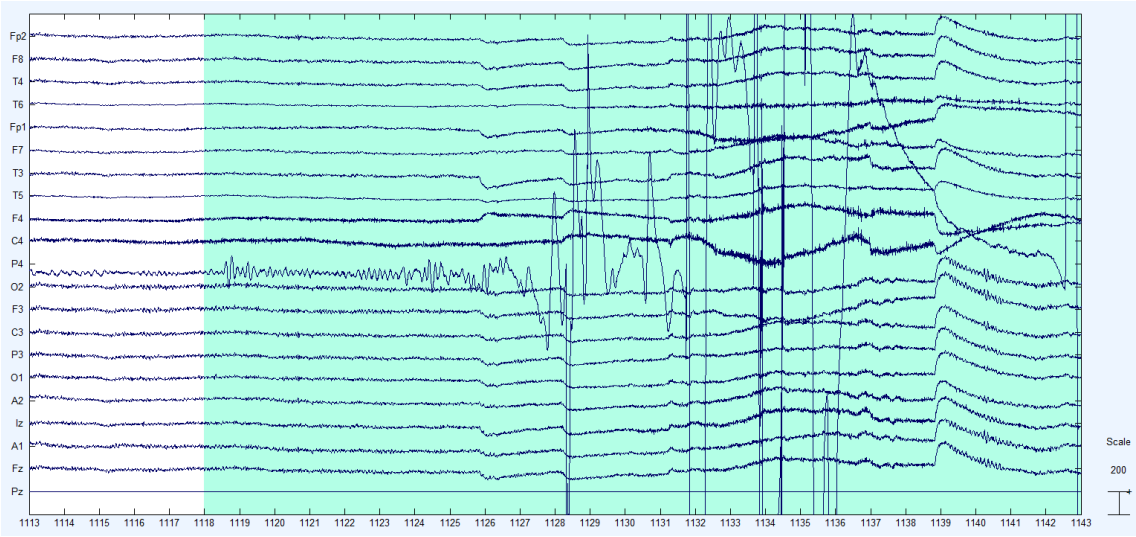

Figure 3.6: High amplitude artifact that clearly overwhelm any EEG. They cannot be left in the data or removed with AAR. This case was also in one channel of interest (F4-C4) , so there was no doubt in removing it.

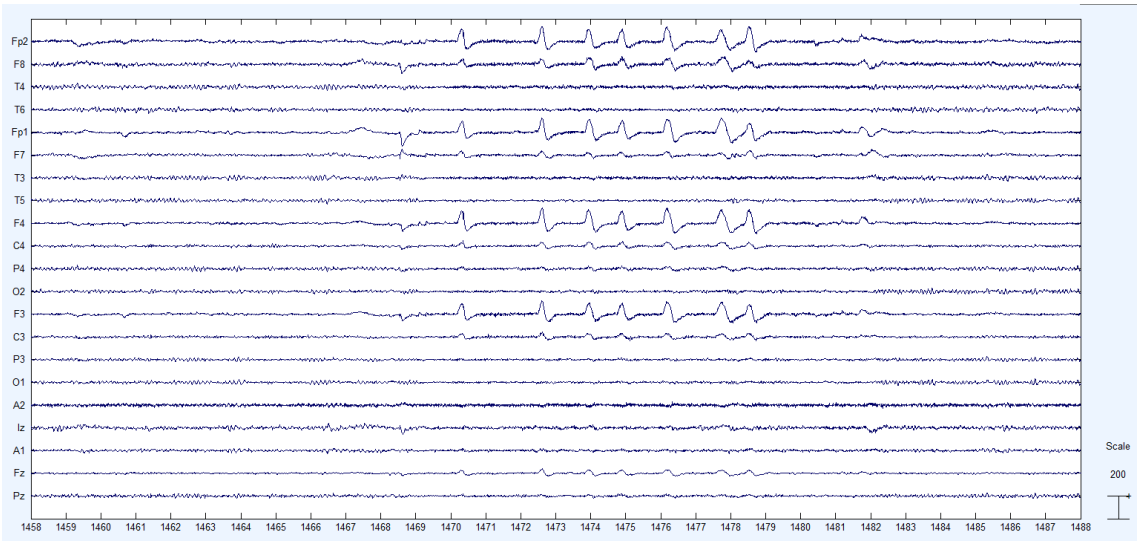

Figure 3.7: An example of blink artifacts in the frontal channels that were not removed, because they should be able to be removed with AAR without removing "good" EEG. Even without the AAR, they do not cause much trouble due to their short appearance and low amplitude.

Table 3.2: Data lengths before and after manual rejection in samples and percentually. Sample frequency is marked as *fs* and the values *NaN* represent the missing values of the corrupted patient data.

Patient		**fs**	**Before**	**After**	**Left**
		Hz	Samples		Percent (%)
2506	Pre	500	306171	151196	49,4
	Post	500	238591	116638	48,9
5570	Pre	500	307022	71236	23,2
	Post	500	265036	82129	31,0
5582	Pre	500	314370	255646	81,3
	Post	500	222987	173246	77,7
5891	Pre	200	308000	250875	81,5
	Post	200	181400	166087	91,6
5952	Pre	500	299292	75142	74,9
	Post	500	248304	225413	90,8
6045	Pre	500	304762	243219	79,8
	Post	200	236800	209731	88,6
6344	Pre	200	327000	266875	81,6
	Post	200	302200	229653	76,0
6373	Pre	200	296600	282675	95,3
	Post	200	239800	216709	90,4
6410	Pre	500	330069	NaN	NaN
	Post	500	248272	NaN	NaN
6423	Pre	200	294000	279696	95,1
	Post	200	236000	222005	94,1

3.4 Notch filter

The data also had some bad characteristics due to the 60Hz notch filter. With the other equipment the notch filter was turned on and with the other off, so the frequency band around 60Hz was not consistent and needed to be left out of the analysis. The problem then was how to validate the incoherent band from the measurements.

Because the 60Hz spike seen in the data is really narrow and the gap left by the notch filter quite broad, the more significant factor is the gap left by the notch filter. The gap can be seen in the figure 3.8 where only the signals with the notch filter ”on” are left. Same figure illustrates the validation for the left out band as two lines which represent the 3dB dips from the ”actual” signal.

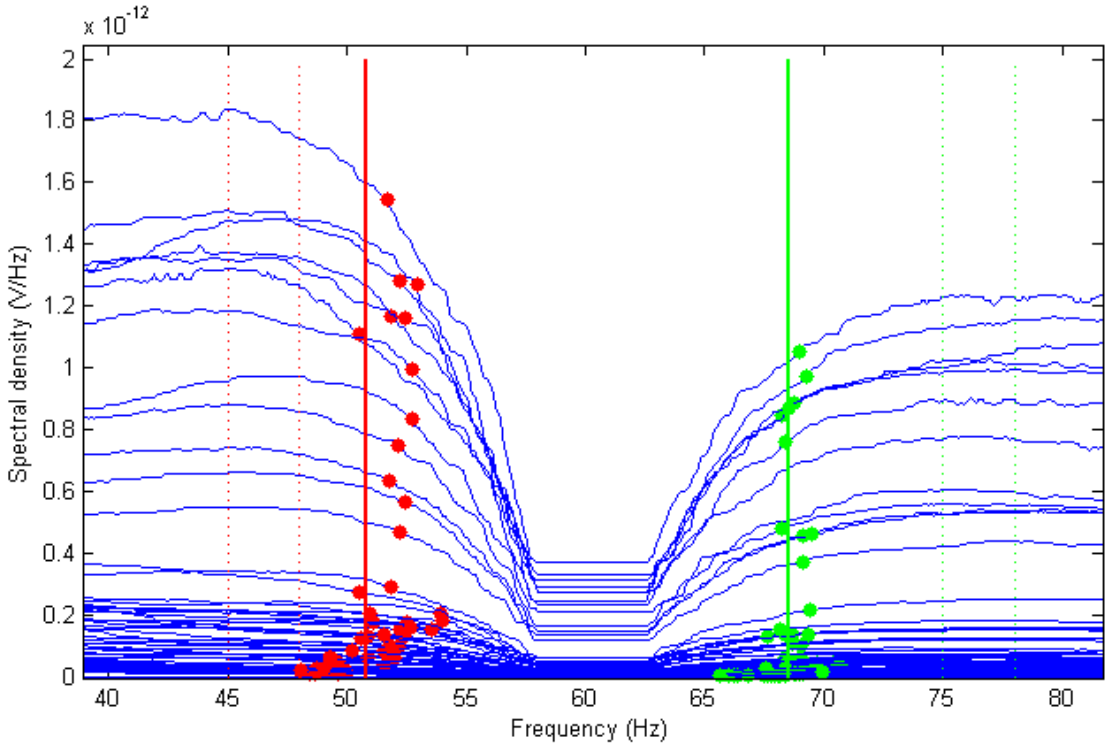

Figure 3.8: Validation of the notch filter band by calculating the 3dB dips from both sides of the gap. The dots represent the 3dB dip of individual signals and the solid lines calculated mean values of those dots.

The dots in the figure represent the 3dB dip for each signal calculated by taking a mean value of the signal from a band before (45Hz - 48Hz) or after (75Hz - 78Hz) the gap (indicated by the dotted lines). The solid lines are then drawn according to the mean value of these dots from both sides of the gap. Now we get the best estimate for the average 3dB drop frequency for the used notch filter. After the calculations the band was estimated to be from 51 to 68Hz. That band was left out from the analysis by rejecting it from the gamma band. It also restricted the width of the requested 50Hz band to 49-51Hz.

3.5 Artifact Rejection

After manual rejection the data was clean from significant artifacts, but there were still a lot of blinks, EOG, and some EMG patterns. These artifacts could be removed using ICA, because they should have a clear source and they are not strong enough to distort the EEG. The ICA and ICA−based AAR are explained in the following subsections.

3.5.1 Independent Component Analysis

ICA is a statistical and computational technique for discovering the independent components from a seemingly random data [19]. In EEG measurements it can be used to find the individual artifact signals from a multichannel EEG recording. Although the EEG looks random, and for the EEG part it mostly is, the artifact signals that originate from the body have distinct patterns and are recorded slightly differently throughout the EEG leads. This makes it possible to distinguish them from the EEG.

A common way to describe this is with a cocktail party where there are certain amount of people (neurons/artifacts) and certain amount of microphones (EEG leads). If they are in the same room and there are no echoes or delays, the ICA can identify the signals of individual speakers. When analyzing the EEG data, the ICA can identify distinct EEG pattern or artifacts and even locate them. This makes it possible to remove the unwanted patterns, or modify them, to clean the data. Figure 3.9 illustrates this with two speakers and two microphones. [22]

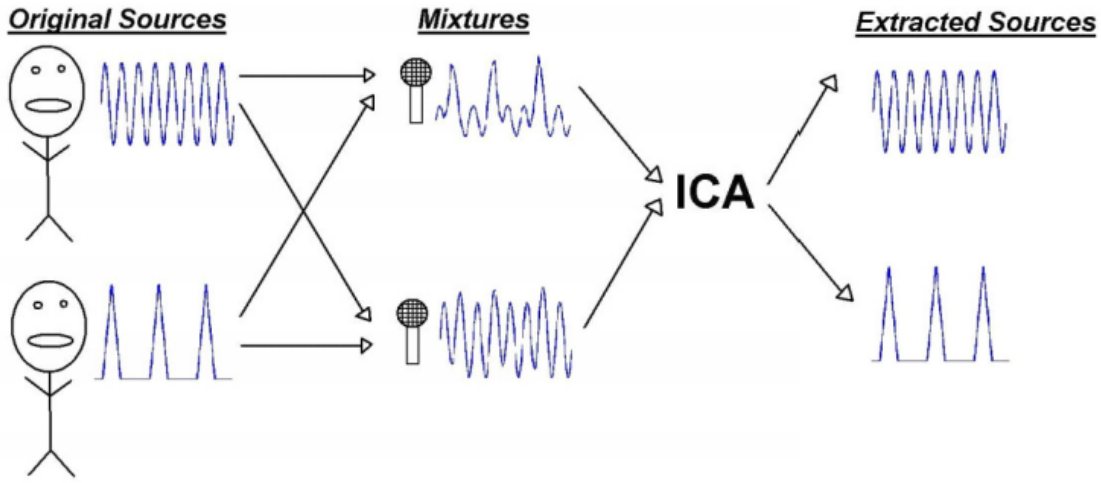

Figure 3.9: ICA can decompose the original signals from two recordings and two sources [22].

The ICA model assumes the data variables to be linear mixtures of unknown latent variables, and the mixing system to be unknown. The latent variables are also assumed to be nongaussian and mutually independent [18]. If we take a random observed vector $\mathbf{X} = [X_1, X_2, ..., X_m]^T$, whose m elements are mixtures of m independent elements of a source vector $\mathbf{S} = [S_1, S_2, ..., S_m]^T$ given by

$$\mathbf{X} = \mathbf{AS}. \tag{3.1}$$

Where $\mathbf{A}$ represents an $m \times m$ mixing matrix. The goal of ICA is to find the

unmixing matrix $\mathbf{W}$ that will give $\mathbf{Y}$, the best possible approximation of $\mathbf{S}$ [22]:

$$\mathbf{Y} = \mathbf{WX} \cong \mathbf{S}. \tag{3.2}$$

In this work, the ICA is used as a part of AAR to recognize the unwanted artifacts from the EEG. The artifacts are then automatically removed from the mixing matrix $\mathbf{A}$ and the signal reconstructed without the artifacts.

3.5.2 Automatic Artifact Rejection

AAR is a wide term but in this context it is an ICA-based automatic artifact rejection algorithm by MSc Narayan P Subramaniyam from the Tampere University of Technology, Department of Electronics and Communications Engineering [40]. The algorithm automatically identifies the artifactual independent components (AIC) containing artifactual activity (EOG or EMG) based on fractal dimensions (FD), and then uses a fractal based wavelet denoising method along the lines of wICA to denoise the automatically identified AIC [40]. The method (F-wICA) differs from wICA, presented as a superior technique in the literature review, in two aspects: It uses stationary wavelet decomposition and fractal-based wavelet thresholding only for automatically identified AICs [40].

At the time of this thesis the algorithm was not ready and could not be used for the "actual" analysis. A lot of time was used to evaluate the algorithm along with Subramaniyam and although it seemed to work, it still erased too much of the actual data, the same problem Cassani et al. found with ADJUST and FASTER algorithms [8].

The algorithm takes in the ICA components, window length, and the wanted artifact to be removed. ICA components were obtained with EEGLAB SOBI method [3], same as Tran et al. used for their data, because it has been used to identify ocular sources [42]. Window length was used to determine the length of the data segments used and wanted artifact parameter affected the artifact the algorithm searched for and erased.

From the windows of data the algorithm looks for artifacts and erases them from the components themselves. When the data is again reconstructed with the mixing matrix, the data should be clear of artifacts. The wanted artifacts were "EOG" and "EMG", in this context, because the data had some huge EMG distortions, as can be seen in Figure 3.5, and also a lot of EOG patterns, as can be seen in Figure 3.7.

The algorithm compares the fractal values of the components and removes the component with the highest value. The window lengths for the different artifact rejections need to be chosen carefully because they might affect the result quite a bit. There are no clear guidelines for the selections but only word of mouth knowledge.

It is often advised that with EMG one should use longer window lengths, like 30 seconds, and with EOG a bit shorter, like 10 seconds.

Most of the time evaluating the algorithm was used in deciding the window lengths. The results are so case sensitive that it took time and was really hard to evaluate. Finally we chose to make a complex and time consuming script, which tried different window length for both EMG and EOG and saved the band powers of every channel. This way we could graphically analyze the effect of the window length in relation to the power spectrum values. The results for one channel (Fz-Cz) can be seen in Figure 3.10.

Figure 3.10 shows that EOG artifact rejection removes a lot of data from all the bands. Although, its effect on the interesting beta bands is quite mild compared to the other bands, its effect on the gamma band raises the concerns. By its nature EOG has low frequency values so it should not be affecting higher bands, such as the gamma band. But as can be seen in the subplot for the gamma band, the algorithm removes significant amounts of data. It is quite fair to state that this behavior of the algorithm is faulty.

According to the figure, the EMG artifact rejection looks quite valid. It removes data from all the bands, which is a normal behavior, because EMG affects on a broad spectrum. The effect of the window length can also be seen really nicely. It seems that the longer the window length the more is rejected. This happens because the algorithm removes longer segments of the data according to the window length. On average longer segments contain more valid data than artifacts, so some huge EMG artifact in a long data segment (window) make the whole segment to be rejected.

Alone the EOG artifact rejection raised such concerns, that it was decided not to use the AAR algorithm on its current state. The problem of the algorithm might be that currently it assumes that the segment it is processing contains even one artifact. This makes it to remove some valid data as "artifacts". The author of the algorithm is aware of the problem and making changes to it.

By the time the problem was discovered, so much work was done with the algorithm, that it was decided to include the analysis in this thesis. The results are now also composed with the algorithm in addition to the manual rejection, as can be seen from the flow chart in the Appendix C. The results should then be invalid, but it is educating to see how the algorithm evaluated as "faulty", affects the results. The discussion section unfolds this topic.

3.6 Data processing

After the data conversions and artifact rejections the data needed to be processed for the final presentations. There were 21 channels of EEG from pre and post measurements of eight patients. Those files needed to be processed and compressed

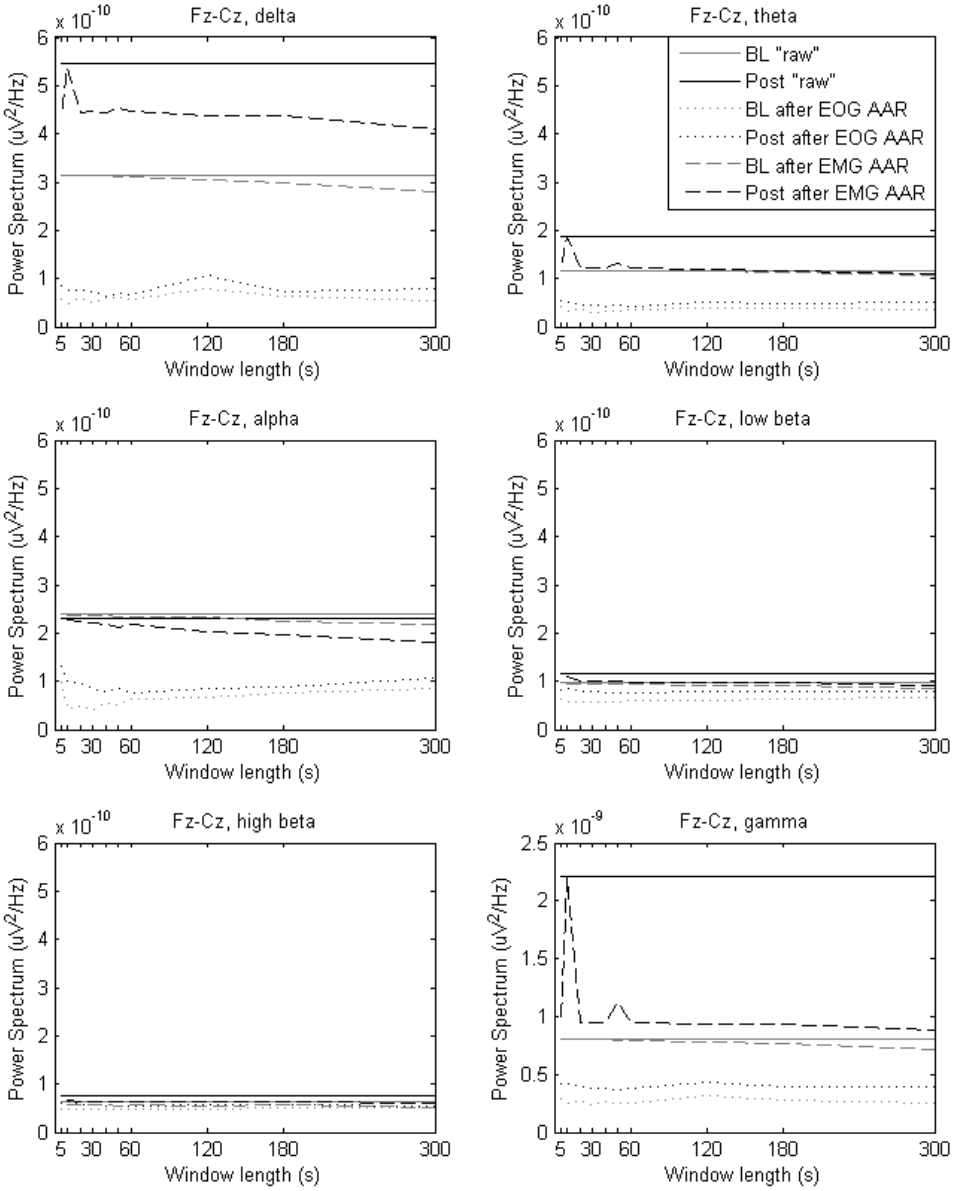

Figure 3.10: The effect of AAR window length in relation to the power spectrum values. One subplot consists of a sum of pre and post measurements of all patients on one channel (Fz-Cz). Pre and post measurements are further divided into "raw" baseline value and after EOG and after EMG rejection. EOG artifact rejection seems to remove a lot of data from all the bands. EOG artifact has low frequencies, so rejecting it should not be affecting higher bands, such as the gamma band. But as can be seen in the subplot for the gamma band, the algorithm removes significant amounts of data. It can also be seen that the longer the window length the more data is rejected. This happens because the algorithm removes longer segments of the data according to the window length.

into one file. This process is included in the script called "final_script" which can be found in appendices from A to C.

The data processing meant that we needed to calculate the power spectrum densities of seven bands (Delta, Theta, Alpha, Low Beta, High Beta, 50Hz, and Gamma) and save the results into matrices. The power spectrum densities were calculated using the Welch's method with the Matlab function *pwelch* [28]. The function returns the power spectral density (PSD) estimate, of the input signal, using Welch's overlapped segment averaging estimator [28]. Parameters for the pwelch were 200Hz sampling frequency, 2048 of FFT points, 50% overlap and 2000 sample window length. From minutes of data the pwelch function computes the bands by sliding a window through the data and calculating the average power spectrum. Note that small and short artifacts in the data do not affect the results much when the average is taken from minutes of data, like in this thesis.

When the PSD estimates were calculated for each patient they were saved into two matrices from which they were again compressed into one file. That file then included all the compressed data from all the patients. That file was then used to construct the results presented in the next sections.

3.7 Graphical result analysis

Apart from the AAR algorithm evaluation, a lot of work was done for the presentation of the data for the result analysis. Like said before, the data was highly corrupted and hard to clean. In this case, even after the clean up the results are not quite clear because there are still too few patients to analyze and they are measured with two equipments.

This changed the initial plan that the data could be presented with Matlab box plots, which "present the data as a box with center mark as the median and edges of the boxes as 25th and 75th percentiles with whiskers extending to the most extreme data points" [27]. Box plots work well with large datasets, but with smaller amounts of data the individual data points become too significant and meaningful distorting the plot and so forth the results. With finally datasets of four patients each, the boxplot is out of the question.

Four data points is actually too small to present the data in any grouped form, because the significance of an individual value is too high. So the only way to present the data graphically is to present the results individually. Because an individual result consists of two points (pre-post), one way is to present the change as a line. The line should then intuitively suggest the trend and magnitude of the change between the two results. Fortunately eight lines can be presented quite nicely in one graph and with such a small width, even the seven channels (Delta, Theta, Alpha, Low-Beta, High-Beta, 50Hz, and Gamma) can be presented in one figure.

This led to the conclusion that the data was presented as individual line graphs in the same subplots, with six subplots presenting the interesting channels as one figure. These figures (from 4.1 to 4.3) should be quite intuitive to read because the lines can be read seperately but also the trend of a group of lines is visible.

3.8 Statistical analysis

Along with graphical analysis the data should be statistically analyzed to find if the results are significant enough to be valid. Because the amount of patients (n=8) was so low, it was not known if we could analyze the data statistically. For this reason we decided to consult statistician Mika Helminen from University of Tampere.

He informed us to make a nonparametric test, due to low n-value and also because the n-value was below 10, we could not make a normality test. He advised us that Wilcoxon signed rank test would be the best approach for our data and if the test indicates statistically significant results (P-value $<$ 0,05), they really should be significant. He also said that if the results are not statistically significant, the treatment really did not work or there was just not enough patients to be sure.

The Wilcoxon signed rank test is a nonparametric test, which does not assume normality in the data and can be used when the dependent t-test is inappropriate. Wilcoxon test is used to compare two sets of values from the same patients, which is exactly our case. [39]

The Wilcoxon test can be used when two criteria are met [39]:

1. The dependent variable is measured at the ordinal or interval/ratio level
2. The independent variable consists of two categorical, "related groups" or "matched pairs".

The first criterion is met by calculating the power spectra of the bands as numerical values. The values are then comparable, because they are obtained the same way. One might argue about the comparability of the values, since they are based on the physical measurements on different time frames and conditions. However, in order to make any kinds of measurements and studies, these problems need to be accepted and minimized. In our case the conditions do differ a lot between patients, but not so much between the pre and post measurements of individual patient. The second criterion is met by "matched pairs", which the patients represent as themselves, because the pairs are formed from pre and post measurements. The effect of the study should then be between these pairs.

The Wilcoxon signed rank test was done using a Matlab function *signrank* [29]. Results of the Wilcoxons signed rank test can be seen in Tables 4.1, 4.3, and 4.5.

4. RESULTS

Results consist of three sections. They present the results from three different artifact rejection "cases" (raw, manual, and manual and AAR) and are used to discuss the effect of the rejection method.

The sections are further divided into tree presentation forms, which include a table of the results from the Wilcoxon signed rank test, a table of the change trends that occurred in the results, and a figure of subplots of the power spectrum changes from pre to post measurements for each patient. The second section, which presents the results of the manually rejected data, is the one used to evaluate the effect of the treatment, because it was evaluated (in chapter 5) to be the most accurate way the reject the artifacts.

4.1 Raw data

Raw data was left intact, so it contains some heavy artifacts and fluctuations. In one sense the data represents the conditions the best, but because the EEG signals fluctuate so much and have undesired components in them, the pre and post measurements are really not that comparable.

The first Table 4.1 includes the P-values of the Wilcoxon signed rank test. There are tree bands that seem to be significantly changed, but they are not in the channels or bands of interest. The channels are located next to one another in the right backside of the brain, so the results are local. This seems really interesting, but it really becomes significant if the following sections indicate the same. Now the huge changes in EEG due to artifact may affect too much. The effect can be seen in the gamma band, where the P-values are almost the same throughout the channels. This can also be seen in Table 4.2, where the changes are the same. The gamma band may contain really bad EMG bursts (Figure 3.6), so huge artifacts in some measurements may affect the whole results, as they seem to have in this case.

The second Table 4.2 includes the number of positively, according to the hypothesis, changed patient results. It is merely obtained to support the Table 4.1, so that it should indicate whether the significantly changed results are changed in the right direction. Like said before, with this "raw" dataset it indicated that tree significant results had changed in the wrong direction and outside the hypothesis.

Table 4.1: P-values for the raw data using non-parametric paired Wilcoxon test. Gray cells are the channels and bands of most interest and yellow cells indicate the significant cells below the significance level 0.05 other than them.

	Delta	**Theta**	**Alpha**	**Low Beta**	**High Beta**	**50 Hz**	**Gamma**
	1-4Hz	**4-8Hz**	**8-12Hz**	**12-20Hz**	**20-30Hz**	**49-51Hz**	**30-49 - 68-100Hz**
Fp2-F8	0,383	0,195	0,547	0,547	0,461	1,000	0,313
F8-T4	0,844	0,844	0,313	1,000	0,844	0,742	0,313
T4-T6	0,383	0,148	0,008	0,250	0,742	0,844	0,313
T6-O2	0,250	0,148	0,008	0,195	0,109	0,844	0,313
Fp1-F7	0,641	0,461	0,641	0,844	0,742	1,000	0,250
F7-T3	0,742	0,148	0,461	0,313	0,641	0,742	0,250
T3-T5	0,461	0,195	0,250	0,383	0,313	0,945	0,313
T5-O1	0,461	0,313	0,250	0,742	0,641	0,461	0,313
Fp2-F4	0,641	0,383	0,313	0,844	0,742	0,383	0,313
F4-C4	0,383	0,742	0,945	0,641	0,844	0,547	0,313
C4-P4	0,109	0,250	0,109	0,109	0,148	0,844	0,313
P4-O2	0,383	0,148	0,195	0,547	0,844	0,945	0,313
Fp1-F3	0,547	0,461	0,945	0,844	0,641	0,742	0,313
F3-C3	0,945	0,844	0,844	1,000	0,945	0,945	0,313
C3-P3	0,641	0,383	0,148	0,055	0,195	0,742	0,313
P3-O1	0,547	0,461	0,461	0,742	0,945	0,945	0,313
A2-T4	0,547	0,008	0,250	0,641	0,945	0,844	0,313
T4-T3	0,742	0,844	0,641	0,461	0,547	0,742	0,313
T3-A1	0,438	0,438	0,813	0,625	0,625	0,813	0,313
Fz-Cz	0,547	0,547	0,641	0,945	0,461	1,000	0,313
Cz-Pz	0,109	0,109	0,945	0,195	0,250	0,641	0,313

The Figure 4.1 includes subplots of the power spectrum changes from pre to post measurements for each patient. Although the previous tables contain the results and their significance, the figure presents the trends and magnitudes of individual pre to post changes. With a quick glance there is no clear trend but the lines are scattered in both up and down directions. Some changes are quite dramatic between pre and post measurements, but with the raw dataset they may be due to high artifact concentration in either pre or post measurements.

They also indicate one problem with the other equipment, the channel Cz-Pz had significantly lower values than the other. It did not affect the results much, because the results were compared individually between the patients themselves. This supports the fact that one patient needed to be excluded because the results were obtained with two different equipments.

Table 4.2: Number of patients (n/8) where power decreases from pre to post for the raw data. Gray cells are the channels and bands of most interest and yellow cells indicate other results of n<2 and n>6 either positively or negatively changed values.

	Delta	**Theta**	**Alpha**	**Low Beta**	**High Beta**	**50 Hz**	**Gamma**
	1-4Hz	**4-8Hz**	**8-12Hz**	**12-20Hz**	**20-30Hz**	**49-51Hz**	**30-49 - 68-100Hz**
Fp2-F8	6	6	6	4	5	4	5
F8-T4	4	4	5	4	4	2	5
T4-T6	6	6	8	6	4	3	5
T6-O2	6	7	8	5	6	5	5
Fp1-F7	5	5	5	3	3	3	5
F7-T3	3	6	5	4	5	5	5
T3-T5	5	6	6	4	5	4	5
T5-O1	5	6	6	4	4	3	5
Fp2-F4	4	5	6	3	4	2	5
F4-C4	3	4	4	4	3	2	5
C4-P4	6	6	7	6	6	5	5
P4-O2	5	6	6	5	4	4	5
Fp1-F3	5	4	3	4	3	2	5
F3-C3	3	4	5	4	3	4	5
C3-P3	5	6	6	6	6	4	5
P3-O1	5	5	6	4	4	3	5
A2-T4	4	8	6	4	3	3	5
T4-T3	4	4	4	5	5	5	5
T3-A1	3	3	3	3	2	2	5
Fz-Cz	4	4	5	4	5	4	5
Cz-Pz	3	3	5	2	2	3	5

In order for the measurements to be compared to each other with statistical analysis the trends should be consistent, which they are not. The problem with the gamma band discussed before can be seen in the Figure 4.1, since all but one measurement change with relatively same trend, but one changes significantly and affects the results the most. Same kind of incoherence can be seen in other channels too. This affects the first criterion of the Wilcoxon test discussed in section 5.7, because the ratio level of the pre and post measurements is not coherent between the patients. That coherence is what we are trying to obtain with the artifact rejection.

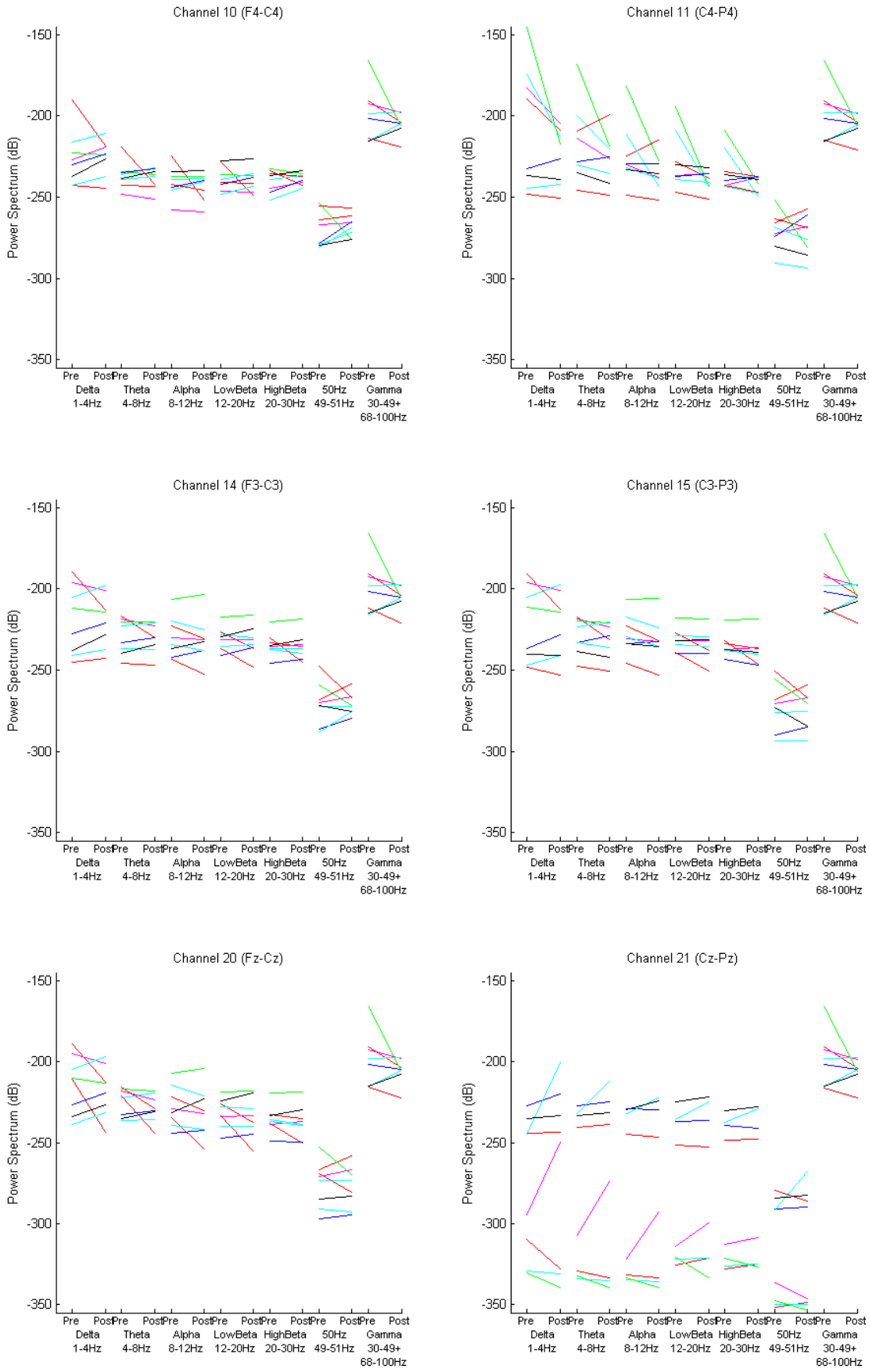

Figure 4.1: Individual colored lines for the power spectrum changes from pre to post measurements for each patient with raw data. Data is divided into seven bands for the six channels of interest.

4.2 Manual artifact rejection

Manual artifact rejection done for the data is explained in detail in section 3.3. It was used to erase the worst artifacts and fluctuations of the data. This makes the data more comparable without affecting the characteristics of the EEG. This method was eventually chosen to be used for the actual analysis apart from the initial manual and AAR rejection, which erased too much real EEG.

The first Table 4.3 again includes the P-values of the Wilcoxon signed rank test. There are several bands in several channels that seem to be significantly changed, but most of them are in channels and bands outside the hypothesis but one. The one significant result occurred in channel F4-C4 on the high beta band, which seems promising for the hypothesis. Also the result for the low beta band is almost significant being 0,078. Looking at Table 4.4 we can see that the significant change occurred favoring the hypothesis, the spectral power rose.

Also all the others but one significance occurred when the spectral power of the band rose from pre to post measurements. This supports the hypothesis well. Especially the spectral powers on both Beta bands rose in channel Fp1-F3, which is a frontal channel as well as the channel F4-C4 that we were interested in.

The second Table 4.4 supports the fact that most of the results occurred in the right direction. Although, in the interesting channels and bands the results are quite neutral, since some changed positively, some negatively and some were neutral.

Table 4.3: P-values for the manually rejected data using non-parametric paired Wilcoxon test. Gray cells are the channels and bands of most interest and yellow cells indicate the significant cells below the significance level 0.05 other than them. The only green cell indicates the one significant result that was in one channel on interest.

	Delta	Theta	Alpha	Low Beta	High Beta	50 Hz	Gamma
	1-4Hz	4-8Hz	8-12Hz	12-20Hz	20-30Hz	49-51Hz	30-49 - 68-100Hz
Fp2-F8	0,148	0,109	0,383	0,078	0,742	0,547	0,195
F8-T4	0,250	0,547	0,547	1,000	0,461	0,641	0,250
T4-T6	0,945	0,383	0,016	0,109	0,461	0,195	0,195
T6-O2	0,945	0,945	0,250	1,000	0,641	0,844	0,195
Fp1-F7	0,461	0,742	0,641	0,547	0,547	0,641	0,250
F7-T3	0,039	0,148	0,383	0,742	0,547	0,844	0,195
T3-T5	0,461	0,945	0,641	0,742	0,844	0,844	0,250
T5-O1	0,945	0,945	0,945	0,461	0,461	0,148	0,148
Fp2-F4	0,547	0,461	0,313	0,148	0,195	0,039	0,078
F4-C4	0,109	0,109	0,250	0,078	0,023	0,008	0,148
C4-P4	0,078	0,461	0,742	0,742	0,547	0,195	0,195
P4-O2	0,844	0,461	0,461	0,547	0,742	0,250	0,195
Fp1-F3	0,148	0,055	0,148	0,039	0,016	0,023	0,109
F3-C3	0,055	0,109	0,547	0,250	0,383	0,547	0,195
C3-P3	0,742	0,641	0,383	0,383	0,945	0,945	0,195
P3-O1	0,641	0,844	0,742	0,148	0,313	0,250	0,195
A2-T4	0,547	0,547	0,945	0,461	0,383	0,742	0,250
T4-T3	0,148	0,195	0,742	0,547	0,641	0,945	0,383
T3-A1	0,313	0,625	1,000	1,000	0,188	0,125	0,109
Fz-Cz	0,383	0,383	0,641	0,547	0,383	0,945	0,195
Cz-Pz	0,078	0,547	0,641	0,313	0,250	0,383	0,195

The trends in Figure 4.2 do not seem as scattered as in previous Figure 4.1 with the raw data, but there are also some inconsistencies. One example is in the channel 21, where the post measurement has significantly higher value than the pre measurement. This cannot be just because of the effect of the treatment. Again with a quick glance there is no clear trend but the lines are scattered in both up and down directions. Although this time there are more upward trends than before. This and the tables representing the manually rejected data do support the hypothesis.

Table 4.4: Number of patients (n/8) where power decreases from pre to post for the manually rejected data. Gray cells are the channels and bands of most interest and yellow cells indicate other results of n<2 and n>6 either positively or negatively changed values. The green cells indicate positively changed results that were in one channel of interest.

	Delta	**Theta**	**Alpha**	**Low Beta**	**High Beta**	**50 Hz**	**Gamma**
	1-4Hz	**4-8Hz**	**8-12Hz**	**12-20Hz**	**20-30Hz**	**49-51Hz**	**30-49 - 68-100Hz**
Fp2-F8	3	2	4	1	3	3	2
F8-T4	2	2	4	3	2	2	3
T4-T6	5	6	7	6	3	1	2
T6-O2	5	5	6	5	6	5	2
Fp1-F7	4	4	3	2	5	4	3
F7-T3	2	3	3	2	3	4	2
T3-T5	3	4	5	4	3	3	3
T5-O1	4	5	4	3	3	2	2
Fp2-F4	3	2	2	1	3	2	1
F4-C4	2	1	2	1	1	0	2
C4-P4	2	4	6	4	4	3	2
P4-O2	4	5	6	6	4	3	2
Fp1-F3	3	1	1	1	1	1	2
F3-C3	1	2	3	2	3	3	2
C3-P3	4	6	5	6	5	4	2
P3-O1	4	4	4	3	3	2	2
A2-T4	3	4	4	3	2	3	3
T4-T3	2	2	5	3	3	4	3
T3-A1	1	2	3	2	1	1	2
Fz-Cz	3	3	3	4	4	4	2
Cz-Pz	1	4	5	2	2	2	2

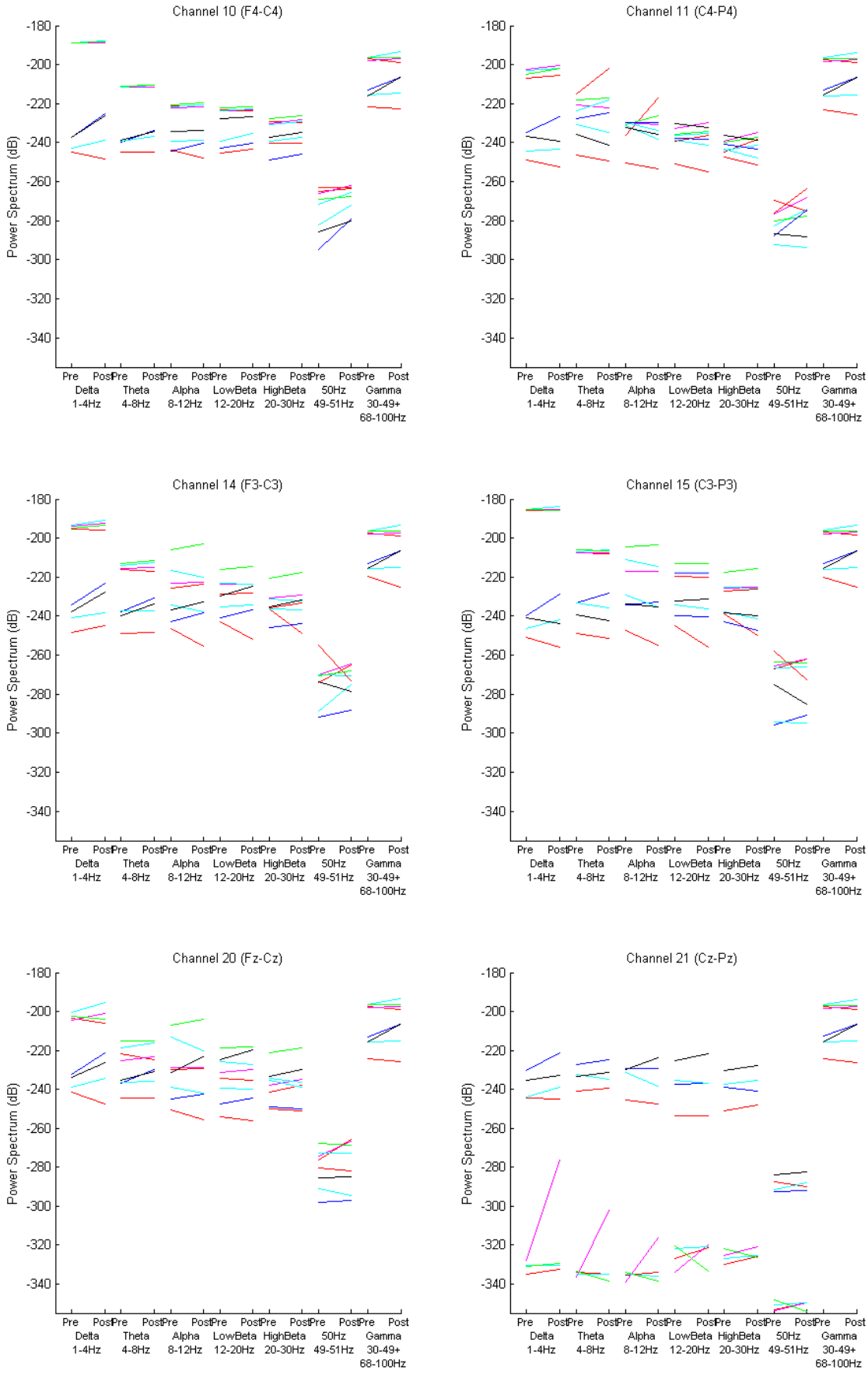

Figure 4.2: Individual colored lines for the power spectrum changes from pre to post measurements for each patient with manually rejected data. Data is divided into seven bands for the six channels of interest.

4.3 Manual artifact rejection in addition to AAR

Manual artifact rejection done for the data is explained in detail in section 3.3 and the AAR in section 3.5. Manual artifact rejection was used to erase the worst artifacts and fluctuations of the data and the AAR was used to erase the remaining EOG and EMG artifacts that were not major and the EEG below salvageable. This kind of rejection method makes the data more comparable without affecting the characteristics of the EEG too much. Unfortunately the AAR algorithm was not ready enough to be used at this point so the method was rejected from the actual analysis. The valuation is explained in more detail in section 3.5.2.

The first Table 4.5 again includes the P-values of the Wilcoxon signed rank test. There are two bands that seem to be significantly changed, but they are not in the channels or bands of interest. The second Table 4.6 indicates that the other occurred in the right and the other in the wrong direction. The one that supports the hypothesis was in channel Fp1-F3, the same as with the manually rejected data.

The second table again supports the fact that most of the results occurred in the right direction. In the interesting channels and bands the results are quite neutral, since some changed positively, some negatively, and some were neutral.

Table 4.5: P-values for the manually and AAR rejected data using non-parametric paired Wilcoxon test. Gray cells are the channels and bands of most interest and yellow cells indicate the significant cells below the significance level 0.05 other than them.

	Delta	**Theta**	**Alpha**	**Low Beta**	**High Beta**	**50 Hz**	**Gamma**
	1-4Hz	**4-8Hz**	**8-12Hz**	**12-20Hz**	**20-30Hz**	**49-51Hz**	**30-49 - 68-100Hz**
Fp2-F8	0,742	0,945	0,461	0,313	0,461	0,641	0,383
F8-T4	0,195	0,148	0,742	0,844	0,461	0,742	0,383
T4-T6	0,461	0,383	0,250	0,742	0,383	0,383	0,383
T6-O2	0,055	0,023	0,250	0,547	0,461	0,742	0,313
Fp1-F7	0,945	0,742	0,313	0,313	0,250	0,641	0,461
F7-T3	0,844	0,742	0,641	0,742	0,641	0,945	0,461
T3-T5	0,844	0,945	0,383	0,945	0,742	0,945	0,461
T5-O1	0,945	0,313	0,383	0,313	0,461	0,547	0,250
Fp2-F4	0,945	0,844	0,313	0,109	0,109	0,148	0,148
F4-C4	0,313	0,250	0,547	0,078	0,055	0,148	0,250
C4-P4	0,945	0,945	0,547	0,742	1,000	0,547	0,313
P4-O2	1,000	0,313	0,641	0,945	0,641	0,641	0,250
Fp1-F3	0,547	0,109	0,148	0,195	0,109	0,039	0,195
F3-C3	0,195	0,844	0,844	0,742	0,461	0,742	0,383
C3-P3	0,742	0,547	0,461	0,641	0,844	0,844	0,383
P3-O1	0,742	0,844	0,945	0,844	0,383	0,547	0,313
A2-T4	0,844	0,195	0,641	0,313	0,383	1,000	0,383
T4-T3	0,383	0,313	0,945	0,742	0,641	0,945	0,547
T3-A1	0,547	0,641	0,383	0,547	0,250	0,250	0,195
Fz-Cz	0,313	0,313	0,742	0,383	0,195	0,844	0,195
Cz-Pz	0,250	0,641	0,547	0,844	0,461	0,547	0,250

Table 4.6: Number of patients (n/8) where power decreases from pre to post for the manually and AAR rejected data. Gray cells are the channels and bands of most interest and yellow cells indicate the significant cells below the significance level 0.05 other than them.

	Delta	**Theta**	**Alpha**	**Low Beta**	**High Beta**	**50 Hz**	**Gamma**
	1-4Hz	**4-8Hz**	**8-12Hz**	**12-20Hz**	**20-30Hz**	**49-51Hz**	**30-49 - 68-100Hz**
Fp2-F8	5	4	4	2	3	3	2
F8-T4	2	2	3	4	2	3	2
T4-T6	5	5	6	4	2	3	2
T6-O2	7	7	6	6	6	5	3
Fp1-F7	5	4	3	3	2	4	3
F7-T3	4	4	3	2	2	4	3
T3-T5	4	4	5	4	3	4	3
T5-O1	4	5	5	2	3	4	3
Fp2-F4	5	4	2	1	1	2	2
F4-C4	3	3	2	2	2	3	3
C4-P4	4	3	5	5	5	4	2
P4-O2	4	6	5	5	4	4	2
Fp1-F3	4	1	1	2	1	2	2
F3-C3	2	4	3	4	3	3	2
C3-P3	4	5	5	5	5	4	2
P3-O1	4	5	5	4	3	3	2
A2-T4	5	7	3	2	2	3	2
T4-T3	3	3	5	3	4	4	3
T3-A1	3	5	3	3	2	3	2
Fz-Cz	3	3	3	3	3	4	2
Cz-Pz	3	4	5	4	3	3	3

The trends in Figure 4.3 seem even more coherent than in previous Figure 4.2 with the manually rejected data, which is quite intuitive, since the AAR rejects more characteristics off the data. This would not be a problem if we knew that the AAR rejects only the artifacts, but as we know that it also rejects valid data, it is an issue. Another interesting result can be seen in channel Cz-Pz, where the low values have changed their trends in relation to the other results from different rejection methods. It seems that the AAR treats these signals quite dramatically, which might be because of their nature. For having such a low values the signals might be quantisized, so some of their characteristics might be lost in the first place and the AAR only makes it worse.

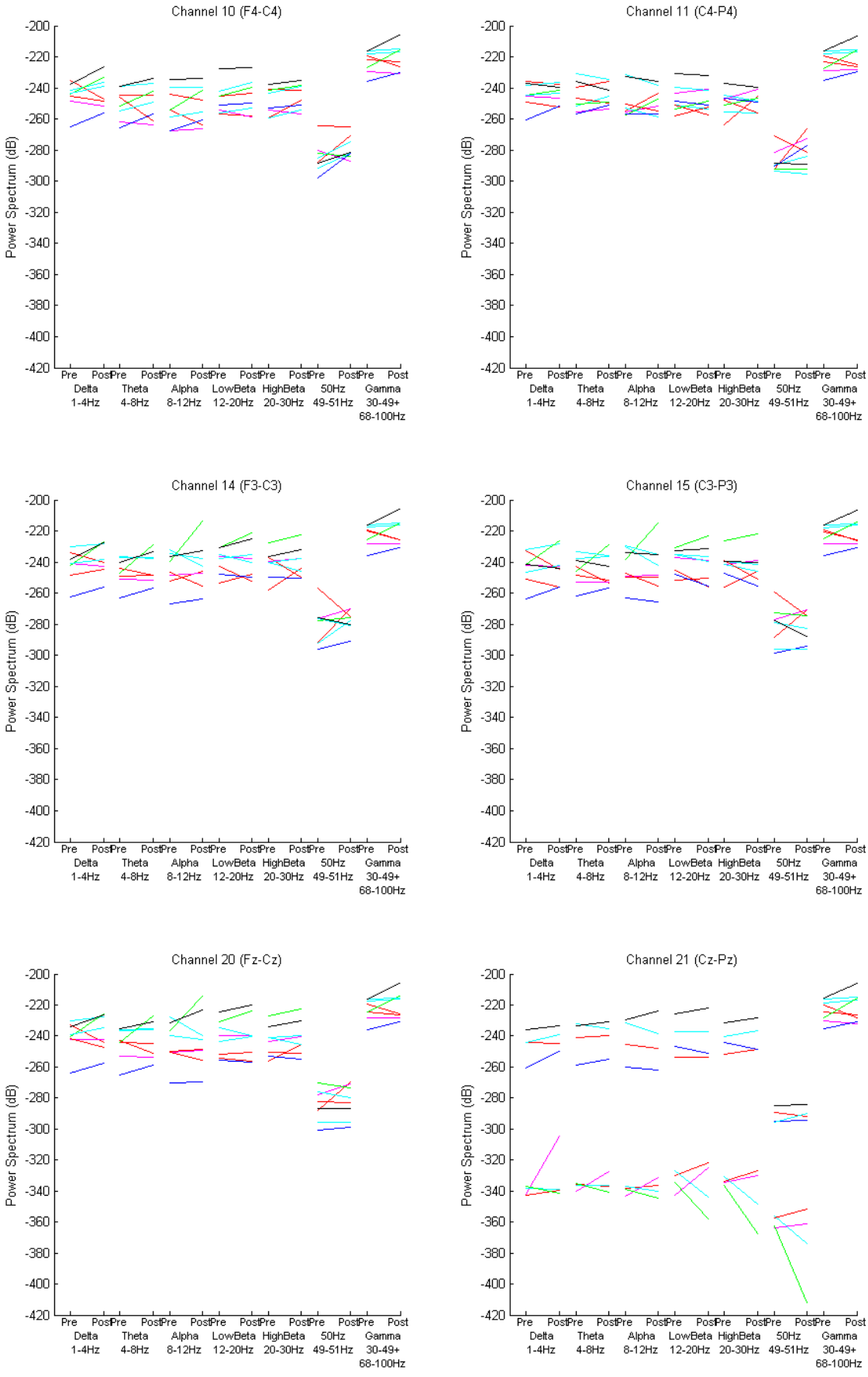

Figure 4.3: Individual colored lines for the power spectrum changes from pre to post measurements for each patient with manually and AAR rejected data. Data is divided into seven bands for the six channels of interest.

5. DISCUSSION

In this study about the effect of the repeated 50 Hz TMS treatment of PD patients it was found that the treatment had some positive effects on the power spectrum densities of the patients. Along with finding the effect of the treatment to the EEG power spectrums a novel AAR algorithm was tested and compared to both raw data and manually rejected data. As the limitations of the study were in such a great part of the study they are presented first and the results thereafter.

5.1 Limitations of the study

The data came from a clinical study by Benninger et al. [6] in 2009. The study was merely a safety study about the 50 Hz rTMS then considered as unsafe. Benninger et al. wanted to see whether the higher frequencies really were unsafe. In their studies it was shown that it was indeed safe to use frequencies even that high.

After the positive results they started to discuss whether there was actually a positive change in the patients conditions. The patients had been monitored with EEG before and after the treatment to find for example epileptiform discharges. Along with behavioral changes these EEG recordings might show the therapeutic results of the treatment, so the data was given for us to analyze.

The biggest problem with the data turned out to be the way it was recorded. As it was not intended to be used for further analysis it was not recorded with such care. The EEG signals contained a lot of artifacts and even worse were recorded with two different equipments. The artifacts made the cleaning of the signals a laborious task and the different equipments made the dataset inconsistent dividing it into two groups according to the equipment used. This narrowed the initial patient count from nine to two groups of four, excluding one individual being recorded with both equipments. The small amount of patients made the statistical analysis almost impossible and undermines the results.

As stated above, also another technique was researched within the framework of this thesis, a novel AAR algorithm made by MSc Narayan P Subramaniyam [40]. It was meant to be used to clean the data from the less influential artifacts. After studying on and trial runs of the AAR algorithm, it became clear that the algorithm was not ready to use. It seemed to reject more artifacts than it was supposed to, which turned out to be due to its assumption on there always being an artifact in

the segment of data it was working on.

5.2 Overall results

The results from the selection of the best artifact rejection method used are quite clear. The raw data was simply too filled with artifacts to be used and the AAR algorithm was not ready, so the best option for assessing the results of the rTMS was manually rejected data. The power spectrum densities of the EEG signals after each artifact rejection method were quite intuitive. The more artifacts were rejected the more consistent the measurements became.

Considering the effect of the rTMS treatment on the patients we must then study the power spectral densities of the EEG with manually rejected data. Tables 4.3 and 4.4 and Figure 4.2 combine the results. According to the hypothesis, the power spectral densities of channels F4-C4, C4-P4, F3-C3, C3-P3, Fz-Cz, and Cz-Pz should rise on the beta band (divided in two).

Looking at Table 4.3 we can see the results (P-values) of the statistical Wilcoxon signed rank test. The table indicates eight different cells (as yellow) where the P-value reached a significance level of below 0.05 (5%). Since the hypothesis was a null hypothesis (H_0), the P-value below 0.05 means that there was a significant change between pre to post measurements not to be explained by chance. The eight cells are from five different channels (T4-T6, F7-T3, Fp2-F4, F4-C4, and Fp1-F3) and bands (Delta, Theta, Low Beta, High Beta, and 50 Hz), which means they are quite scattered throughout the scalp and frequencies. From the eight significant changes only one was in a channel (F4-C4) and band (High Beta) of interest.

Because the Table 4.3 only indicates the significance of the change but not the direction of the change itself, the Table 4.4 was made to aid in the interpretation. Looking at the Table 4.4 we can see that the only significant change occurred in the right direction, the activation rose. This means that only one from the 12 cells of interest gave a positive result, but at least none of them gave negative results.

Given the small population, somewhat scattered results, and only one positive result out of 12 possible we can state that the results are not clearly indicating overall positive results. However, directions of changes in Table 4.4 show that the majority of changes happened in the right direction and glancing at Figure 4.2 shows more positive trends than negative, so there might be some excitation going on.

5.3 Comparison to other research done

Review of literature revealed that the AAR algorithms have been successfully used to reject artifacts from the EEG data even for patients with cortical diseases like AD or PD. Like pointed out by Cassani et al. [8], the top of the line algorithms seem to be

using wICA methods. As the AAR algorithm by Subramaniyam used here is an even more sophisticated version of wICA, the F-wICA, it should work well when ready and may even outperform many of the current leader algorithms. Unfortunately right now it remains uncertain, but the fact that these kinds of automatic algorithms are coming and working makes the artifact rejection much easier and the data more comparable in the future.

The rTMS technique presented here is not a top of the line technique anymore because other pulse trends, like TBS [37], have been shown to outperform the "normal" rTMS. However, the rTMS had been shown to affect the mood and gait of PD patients with lower frequencies [23], so the hypothesis is completely valid.

Follow up studies by Benniger et al. followed the safety study presented here. The other one was a randomized, double blind, sham-controlled study about the effects of the 50 Hz rTMS on PD patients [5] and the other a randomized, double blind, sham-controlled study about the safety and efficacy of iTBS [4]. The rTMS study showed no improvement of motor performance or functional status in PD and the iTBS study appeared to improve mood, but failed to improve motor performance or functional status in PD. However, the thoughts of Thut et al. [41] suggest that the EEG is more accurate measurement technique in discovering the changes after TMS treatment, so the EEG recordings of Benninger et al. should be gone through.

The safety study has been covered here and another Master's thesis made earlier by Cristiana M. A. Ferreira in 2011 [11] covers another. In her work, Ferreira neither found any clear indications about the positive effects of the iTBS treatment done by Benninger et al. [4]. At the time of this thesis it was unclear whether someone had studied the EEG recording of the clinical study of 50 Hz rTMS on PD patients [5], so there were no EEG results to compare on.

6. CONCLUSIONS

The repeated 50 Hz TMS treatment had some positive effects on the power spectrum densities of the PD patients. It was shown with a null hypothesis (H_0) that the brain activity increased in another of the beta bands (High Beta) on one channel (F4-C4) significantly (P-value < 0.05) in the population (n=8), like the study question predicted. However, the significant positive change occurred in only one of the 12 studied power spectrum changes, so the overall results were actually quite minor. Due to our small population and limited results we can conclude that there was no meaningful change in the power spectrum densities on the beta band of the PD patients.

The study whether the AAR algorithm could be used in the artifact rejection process indicates that the algorithm was not ready at the time. The data from the effect of the chosen window length showed that the algorithm erased frequencies that it should not had erased. This lead to the conclusion, that the algorithm could not be used or properly assessed in this thesis.

The concluding results of this thesis are that the EEG can and should be used in assessing the effects of the TMS treatment and the use of an AAR algorithm is highly recommended. The EEG results cleaned with an AAR algorithm are much more accurate and comparable in the future than results obtained with somewhat subjective cognitive studies. This kind of methodology will work well after the EEG has been recorded with care, the population is big enough, and the AAR algorithm is thoroughly tested. As the perfect algorithm has not yet been found the results are not completely comparable but in finding the best algorithm and standardizing it, the results from different TMS studies could be compared and the best TMS pattern found.

REFERENCES

[1] Inc. A.D.A.M. Parkinson's disease. *A.D.A.M. Medical Encyclopedia*, 2011.

[2] A. T. Barker, R. Jalinous, and I. L. Freeston. Noninvasive magnetic stimulation of human motor cortex. *Lancet*, 2:1106–1107, 1850.

[3] A. Belouchrani, K. Abed-meraim, J. F. Cardoso, and E. Moulines. Second order blind separation of temporally correlated sources. *Proc. Int. Conf. on Digital Sig. Proc.*, pages 346–351, 1993.

[4] David H. Benninger, B.D. Berman, E. Houdayer, and N. Pal. Intermittent theta-burst transcranial magnetic stimulation for treatment of parkinson disease. *Neurology*, 76:601–609, 2011.

[5] David H. Benninger, Kazumi Iseki, Sarah Kranick, David A. Luckenbaugh, Elise Houdayer, and Mark Hallett. Controlled study of 50-hz repetitive transcranial magnetic stimulation for the treatment of parkinson. *Neurorehabilitation and Neural Repair*, 10:1096–1105, 2012.

[6] David H. Benninger, Mikhail Lomarev, Eric M. Wassermann, Grisel Lopez, Elise Houdayer, Rebecca E. Fasano, Nguyet Dang, and Mark Hallett. Safety study of 50 hz repetitive transcranial magnetic stimulation in patients with parkinson's disease. *Clinical Neurophysiology*, 10:1–7, 2009.

[7] Hans Berger. Über das elektrenkephalogramm des menschen. *European Archives of Psychiatry and Clinical Neuroscience*, 87:527–570, 1929.

[8] Raymundo Cassani, Tiago H. Falk, Francisco J. Fraga, Paulo A. M. Kanda, and Renato Anghinah. The effects of automated artifact remova lalgorithms on electroencephalography-based alzheimer's disease diagnosis. *Frontiers in Aging Neuroscience*, 6:Article 55, 2014.

[9] Arnaud Delorme and Scott Makeig. Eeglab: an open source toolbox for analysis of single-trial eeg dynamics including independent component analysis. *Journal of Neuroscience Methods*, 134:9–21, 2004.

[10] Cristiana Margarida Alão Ferreira. Eeg analysis workflow. In *PowerPoint presentation*, 2011.

[11] Cristiana Margarida Alão Ferreira. Study of eeg spectral bands from parkinson's disease patients treated with transcranial magnetic stimulation. Master's thesis, Escola Superior de Biotecnologia of the Universidade Católica Portuguesa, 2011.

[12] F. Fregni and A. Pascual-Leone. Technology insight: noninvasive brain stimulation in neurology-perspectives on the therapeutic potential of rtms and tdcs. *Nat Clin Pract Neurol*, 3:383–393, 2007.

[13] The Parkinson Study Group. Levodopa and the progression of parkinson's disease. *The New England Journal of Medicine*, 351;24:2498–2508, 2004.

[14] Birgit Guse, Peter Falkai, and Thomas Wobrock. Cognitive effects of high-frequency repetitive transcranial magnetic stimulation: a systematic review. *Neural Transmission*, 117:105–122, 2010.

[15] Mark Hallett. Transcranial magnetic stimulation and the human brain. *Nature*, 406:147–150, 2000.

[16] Mark Hallett. Transcranial magnetic stimulation: A primer. *Neuron*, 55:187–199, 2007.

[17] Healthwise. What is parkinson's disease? *Parkinson's Disease Health Center*, page 2, 2010.

[18] Aapo Hyvärinen. What is independent component analysis? http://www.cs.helsinki.fi/u/ahyvarin/whatisica.shtml.

[19] Aapo Hyvärinen and Erkki Oja. Independent component analysis: Algorithms and applications. *Neural Networks*, 13:411–430, 2000.

[20] E.M. Khedr, J. C. Rothwell, O. A. Shawky, M. A. Ahmed, and A. Hamdy. Effect of daily repetitive transcranial magnetic stimulation on motor performance in parkinson's disease. *Mov Disord.*, 21:2201–2205, 2006.

[21] G. H. Klem, H. O. Lüders, H. H. Jasper, and C Elger. The ten-twenty electrode system of the international federation. *Recommendations for the Practice of Clinical Neurophysiology*, pages 3–6, 1999.

[22] Dominic Langlois, Sylvain Chartier, and Dominique Gosselin. An introduction to independent component analysis: Infomax and fastica algorithms. *Tutorials in Quantitative Methods for Psychology*, 6:31–38, 2010.

[23] Mikhail P. Lomarev, Sulada Kanchana, William Bara-Jimenez, Meena Iyer, Eric M. Wassermann, and Mark Hallett. Placebo-controlled study of rtms for the treatment of parkinson's disease. *Movement Disorders*, 21:325–331, 2006.

[24] Fumiko Maeda, Julian Paul Keenana, Jose Maria Tormosc, Helge Topkae, and Alvaro Pascual-Leone. Modulation of corticospinal excitability by repetitive transcranial magnetic stimulation. *Clinical Neurophysiology*, 111:800–805, 2000.

[25] Jaakko Malmivuo and Robert Plonsey. *Electroencephalography.* Oxford University Press, 1995.

[26] Nadia Mammone, Fabio La Foresta, and Francesco Carlo Morabito. Automatic artifact rejection from multichannel scalp eeg by wavelet ica. *IEEE SENSORS JOURNAL*, 12:533–542, 2012.

[27] MathWorks. boxplot. http://www.mathworks.se/help/stats/boxplot.html.

[28] MathWorks. pwelch. http://www.mathworks.se/help/signal/ref/pwelch.html.

[29] MathWorks. signrank. http://www.mathworks.se/help/stats/signrank.html.

[30] P. A. Merton and H. B. Morton. Stimulation of the cerebral cortex in the intact human subject. *Nature*, 285:277, 1980.

[31] Andrea Mognon, Jorge Jovicich, Lorenzo Bruzzone, and Marco Buiatti. Adjust: An automatic eeg artifact detector based on the joint use of spatial and temporal features. *Psychophysiology*, 48:229–240, 2011.

[32] Ernst Niedermeyer and Fernando Lopes Da Silva. *Electroencephalography.* Lippincott Williams & Wilkins, 2005.

[33] H. Nolan, R. Whelan, and R. B. Reilly. Faster: Fully automated statistical thresholding for eeg artifact rejection. *J Neurosci Methods*, 192:152–162, 2010.

[34] Suomen Parkinson-liitto. Taudin yleisyys. *Vastasairastuneen tietolehtinen 05*, 2005.

[35] Juhani Partanen. *Kliininen Neurofysiologia*, volume 1. Duodecim, 2006.

[36] William Dauer; Serge Przedborski. Parkinson's disease: Mechanisms and models. *Neuron*, 39:889–909, 2003.

[37] Kasper Schindler, Thomas Nyffeler, Roland Wiest, Martinus Hauf, Johannes Mathis, Ch.W. Hess, and René Müri. Theta burst transcranial magnetic stimulation is associated with increased eeg synchroniztion in the stimulated relative to unstimulated cerebral hemisphere. *Neuroscience Letters*, 436:31–34, 2008.

[38] Leif Sörnmo and Pablo Laguna. *Bioelectrical Signal Processing in Cardiac and Neurological Applications.* Elsevier Inc., first edition, 2005.

[39] Leard Statistics. Wilcoxon signed-rank test using spss. https://statistics.laerd.com/spss-tutorials/wilcoxon-signed-rank-test-using-spss-statistics.php, 2013.

[40] Narayan Puthanmadam Subramaniyam and Jari Hyttinen. Fractal based wavelet-ica method for automatic artifact rejection in scalp eeg. Poster, https://events.kuoni-dmc.com/ei3/images/BACI13/Poster/P1/Poster020.pdf, 2013.

[41] Gregor Thut and Alvaro Pascual-Leone. A review of combined tms-eeg studies to characterize lasting effects of repetitve tms and assess their usefulness in cognitive and clinical neuroscience. *Brain Topography*, 22:219–232, 2010.

[42] Yvonne Tran, Ranjit A. Thuraisingham, Ashley Craig, and Hung Nguyen. Evaluating the efficacy of an automated procedure for eeg artifact removal. *31st Annual International Conference of the IEEE EMBS*, 2009.

[43] J. Yianni and T. Aziz. Surgical treatment of parkinson's disease. *ACNR*, 2:21–22, 2003.

A. APPENDIX: FLOW CHART FOR THE ANALYSIS OF RAW DATA

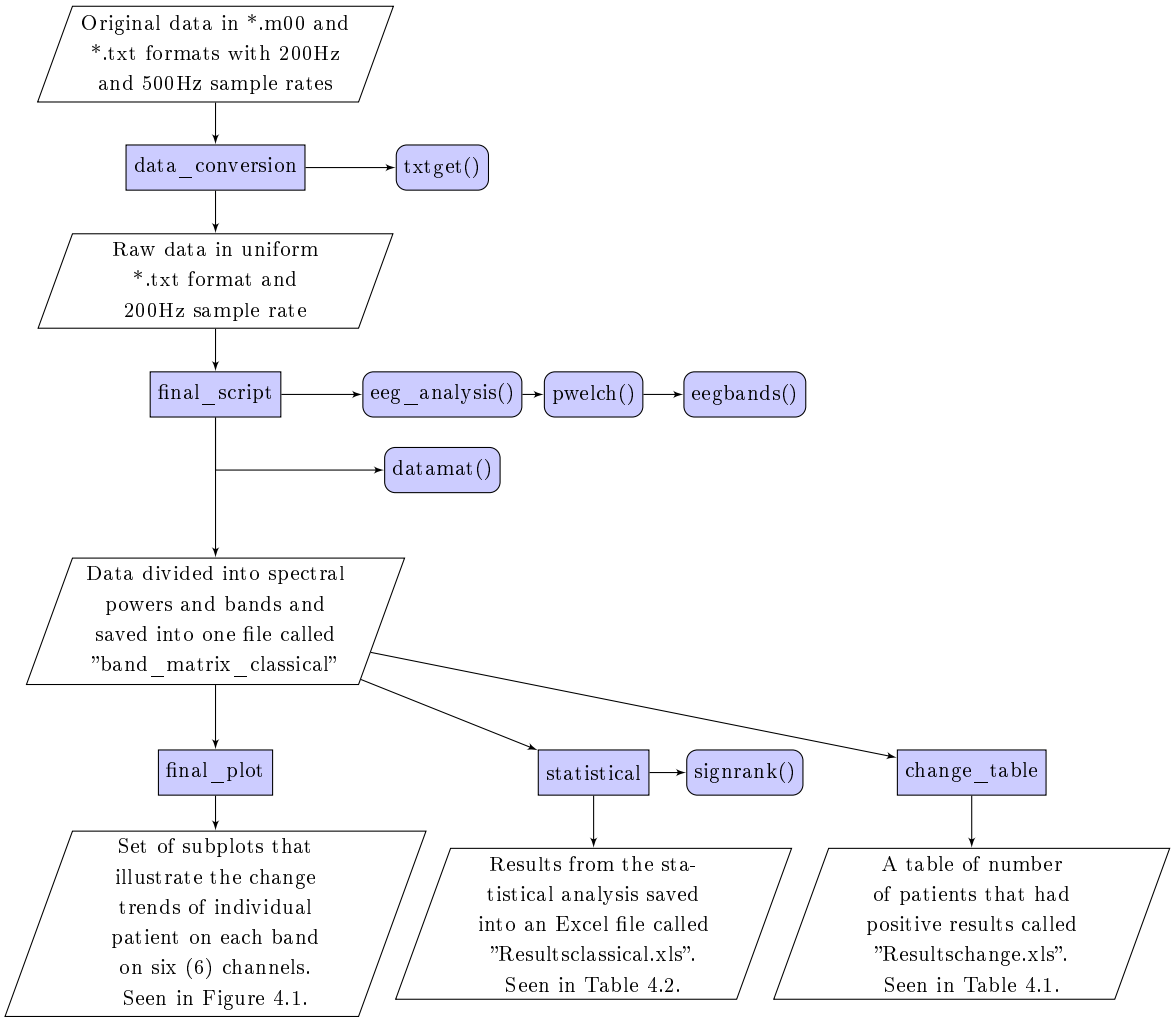

B. APPENDIX: FLOW CHART FOR THE ANALYSIS OF MANUALLY REJECTED DATA

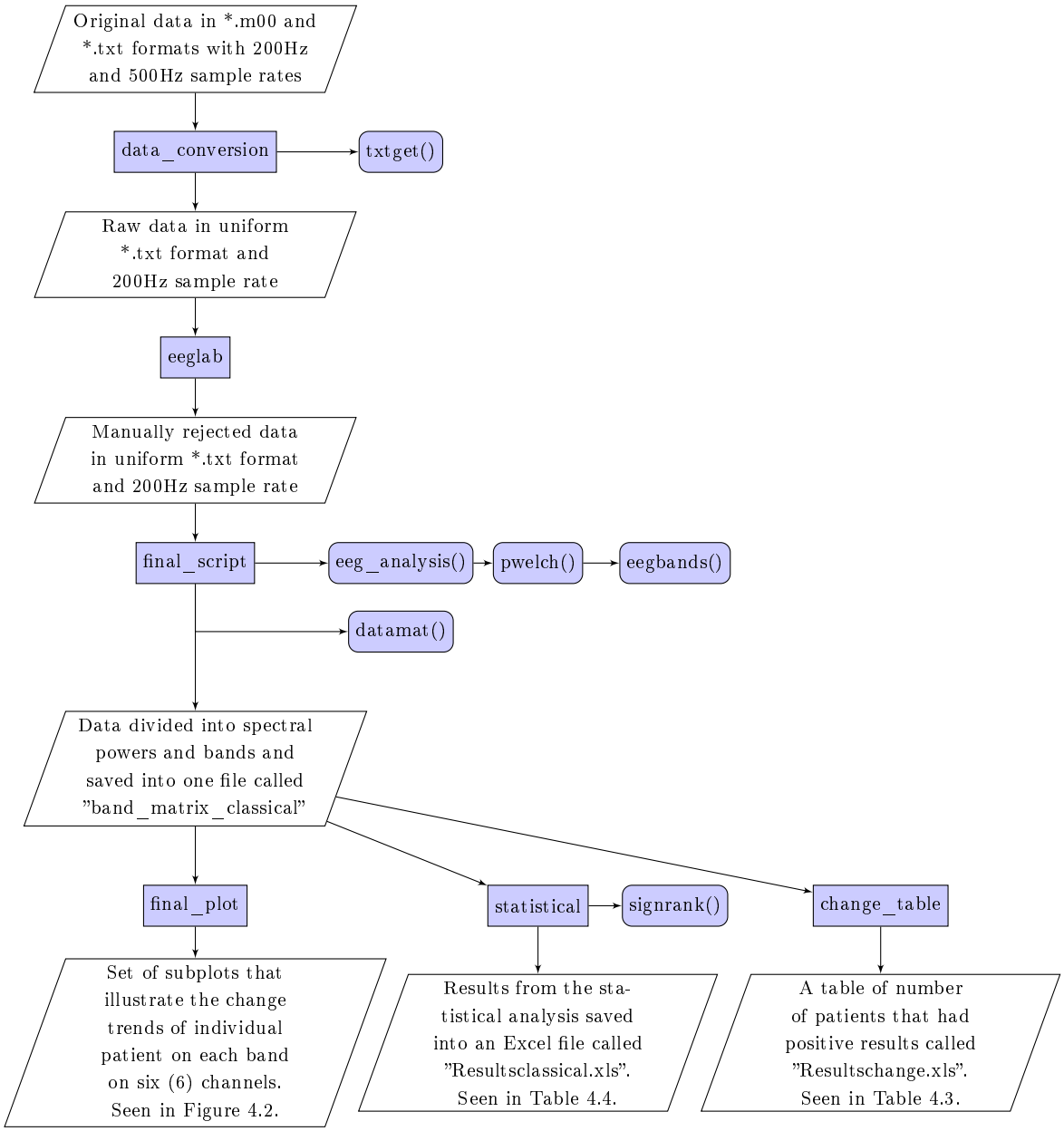

C. APPENDIX: FLOW CHART FOR THE ANALYSIS OF MANUALLY AND AAR REJECTED DATA

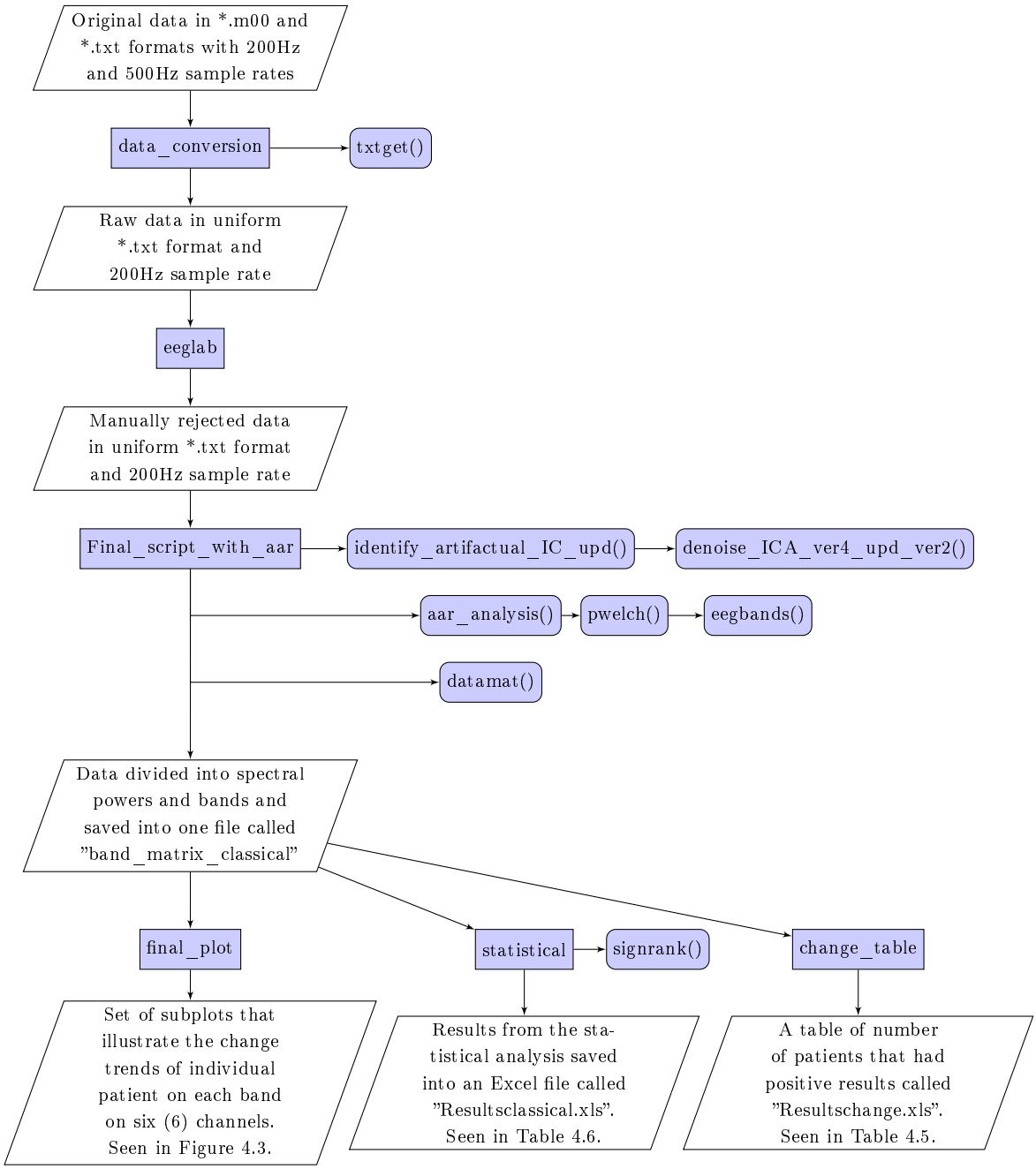

D. APPENDIX: FLOW CHART FOR THE AAR WINDOW TEST